Dissecting the dynamics of cell death pathways in Hirschsprung's Disease: A comparative analysis of viable and non-viable cells under proinflammatory conditions

Dissertation

zur Erlangung des akademischen Grades eines
Doktors der Medizin (Dr. med.)

an der

Medizinischen Fakultät der Universität Hamburg

vorgelegt von

Zhongwen Li

aus

Liaoning/China

2025

Betreuerin der Dissertation: Prof. Dr. Christian Tomuschat

Gutachter:in der Dissertation: Prof. Dr. Ansgar W. Lohse

Vorsitz der Prüfungskommission: Prof. Dr. Ansgar W. Lohse
Mitglied der Prüfungskommission: Prof. Dr. Irwin Reiss
Mitglied der Prüfungskommission: Prof. Dr. Frank Ückert

Datum der mündlichen Prüfung: 18.12.2025

Table of Contents

1. Presentation of the publication

1.1 Introduction

Hirschsprung Disease (HSCR) is a congenital disorder characterized by a lack of ganglion cells in the enteric nervous system, affecting approximately one in 5,000 live births (Austin 2012). This condition leads to considerable gastrointestinal problems due to neuroblasts failing to migrate during embryonic development, resulting in various clinical symptoms based on the extent of intestinal involvement (Bernstein et al. 2021). The primary treatment involves surgically removing the ganglionic section. Nonetheless, genetic factors, especially mutations in genes like the Ret proto-oncogene (RET) and Endothelin receptor type B (EDNRB), add complexity to HSCR's origins (Chen et al. 2021). Additionally, HSCR patients are susceptible to Hirschsprung-associated enterocolitis (HAEC) (d'Aldebert et al. 2020, Gershon et al. 2023, Gunther et al. 2013). Moreover, recent epidemiological studies have reported an increased incidence of inflammatory bowel disease (IBD) among HSCR patients (d'Aldebert et al. 2020, Gunther et al. 2013, Hagens et al. 2022, Ji et al. 2023). These recent studies raise questions such as: Could there be a shared pathophysiology between HSCR, HAEC, and IBD? Do the similarities in apoptotic and necroptotic pathways point to common underlying mechanisms? Are the treatment responses in HSCR and CO cells indicative of broader disease progression connections?

At the molecular level, the receptor interacting protein kinase (RIPK) family, particularly RIPK1 and RIPK3, appears to be a promising target. These kinases are crucial for maintaining intestinal barrier integrity and regulating cell death mechanisms. The signaling pathways mediated by RIPKs, which shift from cell survival to apoptotic (RIPK1-dependent) or necroptotic cell death (RIPK3-dependent), may present a connection since dysregulation of these pathways has been documented in IBD (Kondylis et al. 2017).

Using flow cytometry and directly conjugated monoclonal antibodies, we analyzed cell death pathways in patient derived organoid cultures from HSCR patients and controls. To achieve this, we refined an assay to measure various pathways using FACS in organoid cultures(Wong et al. 2020).

Despite known inflammatory vulnerabilities in HSCR, the precise nature of epithelial cell death regulation in response to inflammatory stimuli remains poorly

characterized. This method enabled us to differentiate between cell death mechanisms within cell populations derived from colonic organoids. Consequently, we identified previously unnoticed yet significant small and large cell groups undergoing various stages of RIPK1-dependent apoptosis (RIPK1+), RIPK1-independent apoptosis (Caspase3+), and necroptosis (RIPK3+), in both viable and non-viable cells. Determining whether cells are viable (Zombie $-$) or non-viable (Zombie+) and their respective cell death pathways is critical for diagnosing diseases and understanding their progression. For example, in gastrointestinal diseases, the balance between viable and non-viable epithelial cells significantly affects the intestinal barrier's integrity (d'Aldebert et al. 2020). In this study, we observed that a proinflammatory cocktail containing TNF-α, IL-6, and IL-1β can simultaneously induce multiple forms of cell death within a single cell (Lee et al. 2018). We demonstrated activated pathways exhibiting high levels of RIPK1-dependent apoptosis, RIPK1-independent apoptosis, and necroptosis (Gunther et al. 2013).

1.2 Material and methods

1.2.1 Study population and covariates

The study adhered to the Declaration of Helsinki guidelines and received approval from the Institutional Review Board Hamburg ethics committee (PV5251). Tissues from patients with Hirschsprung's disease (HSCR, n=5) were sourced from surgically removed specimens, exclusively using the proximal ganglionic portion. Control tissues (CO, n=5) were obtained from patients undergoing surgeries unrelated to Hirschsprung's disease, ensuring a balanced comparison (Table 1). The samples were immediately placed in Iscove's Modified Dulbecco's Medium (IMDM, #12440053, Gibco Thermo Fisher Scientific, Waltham, MA, USA), supplemented with 20% fetal bovine serum (FBS, #0500-064, Thermo Fisher Scientific, Waltham, MA, USA) and 1% penicillin/streptomycin (P/S, #PS/B, Capricorn Scientific, Ebsdorfergrund, Germany). Afterward, they were thoroughly washed with sterile Dulbecco's Phosphate-Buffered Saline (DPBS; #37350, Gibco Thermo Fisher Scientific, USA), and the mucosal layer was carefully separated from underlying tissues, then cut into 1–2 mm pieces. Mucosal cells were isolated by incubating tissue slices in IMDM with 5 mM ethylenediaminetetraacetic acid (#15575-038, Invitrogen, Waltham, MA, USA) and 2 mM DL-Dithiothreitol (DTT, #D9779-5G, Sigma-Aldrich, St. Louis, MO, USA) for 20 minutes at 4°, facilitating crypt structure isolation. They were further filtered through a 70 µm cell strainer (#352350, Corning, Corning, NY, USA) and washed in IMDM containing 2% FBS and 1% P/S, as well as Advanced Dulbecco's Modified Eagle Medium (Advanced DMEM, #12491-015, Gibco Thermo Fisher Scientific, USA), which includes 1% 4-(2-hydroxyethyl)-1-piperazineethanesulfonic acid (HEPES, #H3537-100ML, Sigma-Aldrich, St. Louis, MO, USA), 1% GlutaMAX (#35050-061, Gibco Thermo Fisher Scientific, Waltham, MA, USA), and 1% P/S, collectively referred to as 'Adv.+++'. Each washing step was followed by centrifugation at 500 x g and 4°C for 10 minutes. A solution consisting of extracellular matrix in a 1:2 ratio (Cultrex UltiMatrix, #BME001, R&D Systems, Minneapolis, MN, USA) was prepared. The suspension was pipetted as 30 µl droplets into the center of each well in a 24-well plate (#3022521, Sarstedt AG&Co.KG, Nümbrecht, Germany) and incubated at 37°C in 5.0% CO2 for 30 minutes to solidify the Cultrex. Subsequently, each well received 500 µl of Organoid Growth Medium Human (OGM-h, #060610, Stemcell

Technologies, Canada), enriched with 5 mM ROCK-Pathway Inhibitor (ROC, #72302, Stemcell Technologies, Vancouver, Canada), 1% penicillin/streptomycin (P/S), and 0.02% Primocin (#ant-pm-05, InvivoGen, San Diego, CA, USA), with medium changed every 2–3 days.

After 7-10 days, organoids achieved the necessary confluence for passage. For dissociation, the Cultrex dome was mechanically disrupted in Adv.+++, and the cell suspension was centrifuged at 300 x g and 4°C for 5 minutes. Organoids were further broken down by pipetting 30-50 times. Following centrifugation for cell isolation and supernatant removal, cells were resuspended in Adv.+++ and embedded once again using Cultrex following the previously described protocol. Organoids were maintained in OGM-h containing 1% P/S, with the medium replaced every 2-3 days. Daily evaluations were conducted to monitor structural development and ensure their readiness for experimental use.

1.2.2 Preparation of organoids for flow cytometry

Organoids were assigned to two different experimental conditions: acute and chronic pro-inflammatory treatment groups. Within each group, samples were further divided into untreated and treated subsets. The treated subsets received a cytokine cocktail containing TNF-α (#300-01A, PeproTech, London, UK), IL-6 (#200-06, PeproTech, London, UK), and IL-1β (#200-01B, PeproTech, London, UK) at a concentration of 10 ng/ml for each cytokine, as determined by preliminary experiments (Lee et al., 2018). All organoids were cultured in OGM-h until day 5. Thereafter, differentiation was induced by switching the medium to Organoid Differentiation Medium Human (ODM-h, #100-02114, Stemcell Technologies, Vancouver, Canada) with 1% P/S. In the chronic treatment protocol, treated organoids received the cytokine cocktail on days 3 and 5. In contrast, the acute treatment protocol involved administering the cytokine cocktail on days 5, 6, and 7 (Fig. 1). Untreated sub-groups under both chronic and acute conditions received no cytokine cocktail.

For flow cytometry analysis, organoids were detached from Cultrex domes and resuspended in Adv.+++. After centrifugation at 300 x g and 4°C for 5 minutes, organoids were broken down into single cells using TrypLE (#12605028, Gibco Thermo Fisher Scientific, Waltham, MA, USA) at 37°C for 4 minutes. Following

incubation, cells were washed with Adv.+++ and centrifuged again at 300 x g and 4°C for 5 minutes. The supernatant was discarded, and cell pellets were stained with Zombie NIR fluorescent dye (#423105, BioLegend, San Diego, CA, USA, dilution 1:2,000) in DPBS for 30 minutes at 4°C in the dark. Cells were then washed in DPBS and fixed using eBioFix intracellular fixation buffer (#00-8222-49, BD Biosciences, San Jose, CA, USA) for 20 minutes at 4°C. Subsequently, cells were permeabilized with 0.25% Triton X-100 (#T8787, Sigma-Aldrich, St. Louis, MO, USA) for 15 minutes at 4°C in darkness. Finally, cells were labeled with anti-RIPK3-Alexa Fluor 488 (clone B-2, #sc-374639AF488, Santa Cruz Biotechnology, Dallas, TX, USA, dilution 1:125) and anti-active caspase-3-BV650 (clone C92-605, #564096, BD Biosciences, San Jose, CA, USA, dilution 1:50) for 20 minutes at 4°C in the dark.

Table 1 Patient characteristics for each sample used in this study

Sample	Gender	age at operation (months)	Trisomy Status	Diagnoses	Median group age
#1	male	3.6	negative	Hirschsprung's Disease	
#2	male	3.8	positive	Hirschsprung's Disease, atrial septum defect, persistent oval foramen	
#3	female	16.9	negative	Hirschsprung's Disease	14.4
#4	female	14.4	negative	Hirschsprung's Disease	
#5	female	14.5	negative	Hirschsprung's Disease	
#6	female	6.2	negative	anal atresia, persistent oval foramen, kidney dysplasia, clubfoot	
#7	female	9.3	negative	anal atresia, atrial septum defect, kidney dysplasia, hemivertebrae, multiple ribs, sacral dysplasia, heel feet	7.3

#8	male	7.3	negative	anal atresia, hypospadia sine hypospadia
#9	male	4.9	negative	ileo-colic invagination
#10	male	12.8	negative	anal atresia, esophageal atresia, ventricular septum defect, fused kidneys, sacral agenesia

Fig. 1

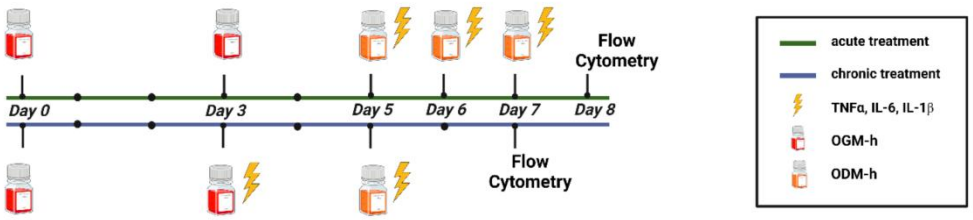

Schematic representation of the experimental timeline detailing the acute and chronic treatment protocols for cell cultures. The green line indicates the timeline for acute treatment, while the blue line represents the timeline for chronic treatment. Cells are treated with cytokines (TNFα, IL-6, IL-1β, indicated by lightning bolts) at specified intervals. OGM-h and ODM-h denote the culture media used during the experiments, with red and orange bottles representing the respective media types. Flow cytometry analyses were conducted on days 5 and 8 to assess the effects of the treatments on cell populations. Organoids from both CO and HSCR were cultured in standard growth medium for five days, followed by differentiation until flow cytometry analysis was performed. This figure was created with BioRender.com

1.2.3 RIPK1-Caspase3-Analysis using flow cytometry

Due to the primary nature of the samples, cell yield limited event count to 10,000 per sample, which we acknowledge as a potential constraint. Flow cytometric analysis was performed on 10,000 individual cells from each subgroup using the BD LSRFortessaTM (BD Biosciences, San Jose, CA, USA). Zombie NIR dye detection was facilitated by a 633 nm laser, with signal collection at 780/60 nm. Caspase3-BV650 fluorescence was identified using a 405 nm laser and collected at 675/30 nm. RIPK3-Alexa Fluor 488 fluorescence was captured by a 488 nm laser and collected at 585/40 nm. Cell debris was excluded by gating based on forward scatter-area (FSC-A) versus side scatter-area (SSC-A) dot plots. Cells were further analyzed on a Zombie NIR versus SSC-A dot plot; all Zombie NIR-positive cells were considered dead. In contrast, Zombie NIR-negative cells, assumed to be viable, were gated on an FSC-A versus SSC-A plot. A more precise distinction between living and dead cells was achieved using Caspase3-BV650 versus RIPK3-Alexa Fluor 488 dot plots. Cells expressing Caspase-3 alone were categorized as undergoing classic (RIPK1-independent) apoptosis, while those positive for only RIPK3 were classified as undergoing necroptosis. Cells positive for both Caspase3 and RIPK3 were interpreted as experiencing RIPK1-dependent

apoptosis. Zombie+ cells negative for both markers were presumed to follow an alternative cell death pathway. Fluorescence minus one (FMO) control were utilized for cell identification, gating, and color compensation. Data were analyzed using FlowLogic software version 8.7 (Inivai Technologies, Victoria, Australia). Each sample was analyzed in technical duplicates across independent runs to ensure reproducibility of staining and gating accuracy.

1.2.4 Light microscopy

Organoids were imaged using a Leica DM IL LED microscope at 4 × magnification. Images were taken directly in their culture wells without fixation or staining to preserve the native structure. Organoids were photographed before and after proinflammatory stimulation at specified time points to observe morphological changes, including crypt structure integrity and signs of cell death. Image analysis was conducted using ImageJ to evaluate structural alterations and overall morphology of the organoids.

1.2.5 Immunofluorescence staining and confocal microscopy

Organoids were fixed in 4% paraformaldehyde, permeabilized with 0.5% Triton X-100, and blocked with 5% BSA to reduce non-specific antibody binding. They were then

incubated with primary antibodies against β-catenin (1:200) and ZO-1 (1:200) overnight at 4°C, followed by incubation with Alexa Fluor-conjugated secondary antibodies (1:500) for 1 h. DAPI (1 µg/mL) was used to stain nuclei. Confocal images were acquired using an Olympus FV 3000 for acute treatment and a Leica SP5 for chronic treatment, at 20 × magnifcation. Z-stack images provided detailed views of the organoid structure, highlighting the localization of β-catenin (red) and ZO-1 (green), with DAPI marking nuclei (blue). Image analysis was performed using ImageJ to assess changes in cellular morphology and junction integrity.

1.2.6 Statistical analysis

Statistical analyses were conducted using GraphPad Prism version 10.1 (GraphPad Software, San Diego, CA, USA). Mean values and standard deviations (SD) were calculated for each data set. Subgroup analyses were performed using paired t tests. A *p*-value less than 0.05 was considered statistically significant. Given the small sample size and the exploratory nature of this study, correction for

multiple testing (e.g., Bonferroni or FDR) was not applied. However, we acknowledge this as a limitation in the interpretation of the results.

1.3 Results

1.3.1 Acute proinflammatory treatment causes increased cell death

The analysis distinguished between non-viable and viable cells by their Zombie-status. Fig.2 shows a significant difference in the proportion of Zombie-positive cells between treated and untreated sub-groups during acute stress. In the HSCR acute group, Zombie+ cells were significantly increased in the treated sub-group (55.39% vs 43.33%, p=0.0229). Similarly, in the control acute group, treated sub-groups had more Zombie+ cells than untreated ones (47.71% vs 34.70%, p=0.009). However, under chronic stress, both HSCR and control groups showed a considerable number of dead cells before and after treatment, with no significant differences (Table 2).

Fig. 2

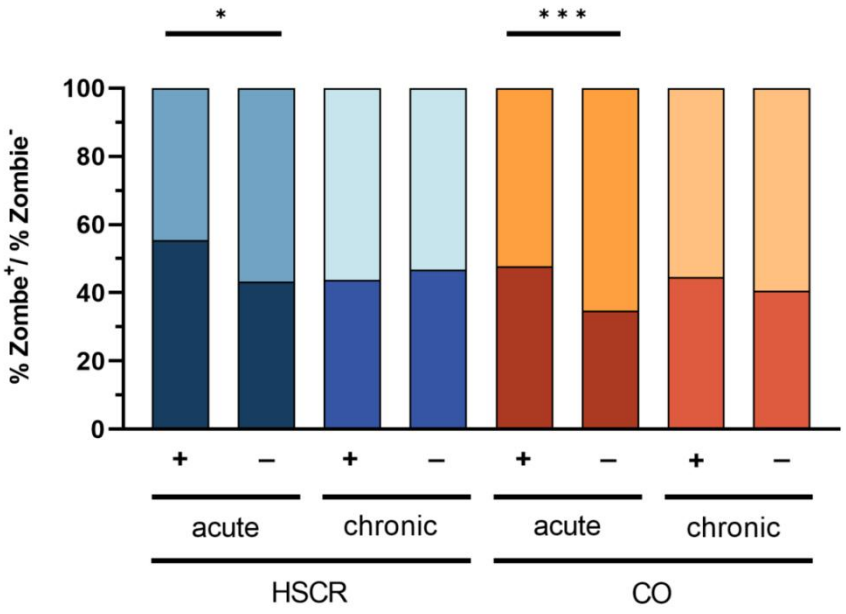

The bar graph shows the percentage of Zombie+ (dead or dying cells) versus Zombie− (living cells) in HSCR and CO cell populations under acute and chronic conditions with and without the specified treatment. The y-axis represents the percentage of cells, while the x-axis compares the different conditions (acute/chronic) and treatments (+/−). Statistical significance is denoted by asterisks (*p<0.05, ***p<0.001), indicating significant differences between the treatment groups. The stacked bars allow for a visual comparison of cell viability across the

different conditions and treatments. The analysis includes 5 organoids for each measured subgroup. The entire cell population was classified based on their zombie stain. Zombie+ cells were identified as dead, while Zombie- cells were considered alive but undergoing cell death. The analysis indicates a significant increase in dead cells following acute proinflammatory stimulation in both HSCR (p=0.0029) and CO (p=0.0009).

Table 2 Summary of Key Findings on the Effect of Treatment on Zombie+ (Dead) Cells in Acute HSCR and CO Groups

Group	Zombie Stain	Analysis Group	Measurement	Key Findings	*p*-value
HSCR	dead (Zombie+)	acute	% dead cells	↑ after treatment	0.0029
CO	dead (Zombie+)	acute	% dead cells	↑ after treatment	0.009

1.3.2 Death cells undergo RIPK1-independent apoptosis after proinflammatory stimulation

RIPK1-dependent apoptosis (RIPK3+/Caspase3+): It was observed as the main cell death mechanism in non-viable cells, as depicted in Fig. 3i. After acute treatment, HSCR organoids exhibited similar levels of double-positive cells (54.88 vs 56.30%, p=0.2825), while chronic stimulation resulted in a notable decrease in double positivity (66.95 vs 56.42%, p=0.0026). Similarly, CO organoids under chronic treatment showed a significant drop in double-positive cells (70.35 vs 60.55%, p=0.0407); however, acute treatment did not demonstrate significant changes, with RIPK3+/Caspase3+ cells decreasing from 58.59 to 50.50% (p=0.2094)

RIPK1-independent apoptosis (RIPK3-/Caspase3+): Independent apoptosis after stimulation for both acute and chronic treatment (14.09 vs 17.11%, p = 0.0220; 12.01 vs. 21.61%, p=0.0158, respectively). While CO cells also presented with this pattern for chronic treatment, increasing from 11.93 to 22.59% (p=0.0159), acute stimulation showed no effect (18.24 vs 21.53%, p=0.3140). HSCR and CO showed similar rates in Caspase3+ cells before and after treatment, as summarized in Fig. 3ii.

Necroptosis (RIPK3+/Caspase3-): Overall, necroptosis was just slightly detectable and showed no significance in HSCR cell death in both treatment regimens (Fig. 3iii). While chronic CO samples appeared similar, acute treatment of controls demonstrated a decline in necroptotic cells posttreatment from 1.66 to 0.50% (p=0.0182).The significant results of all the dead cell analysis are summarized in Table 3.

Analysis reveals that RIPK1-dependent apoptosis is significantly reduced after chronic treatment, while increasing RIPK1-independent apoptotic processes at the same time. Still, RIPK1-dependent apoptosis was more prominent in chronic than in acute treated CO, but not in HSCR. RIPK1-independent apoptosis also increased after acute treatment in HSCR, but not in CO.

1.3.3 Living cells undergo RIPK1-dependent apoptosis after proinflammatory stimulation

RIPK1-dependent apoptosis (RIPK3+/Caspase3+): RIPK1-dependent apoptosis remained the leading cause of cell death in still viable cells, but subgroup analysis was not able to detect significant changes for pre- and posttreatment, as summarized in Fig. 3iv. Following acute treatment, HSCR organoids showed slight decline after treatment (24.69 vs 21.89%, p=0.4065), and chronic stimulation led to a slight rise (34.67 vs 37.12%, p=0.7339). This was also observed for acute and chronic treated CO organoids (25.14 vs 21.46%, p=0.6885; 24.29 vs 26.25%, p=0.5594).

RIPK1-independent apoptosis (RIPK3-/Caspase3+): As shown in Fig. 3v, there was a marked increase in cells undergoing apoptosis in the HSCR acute treated group, ranging from 4.93 to 10.35% (p=0.0474), a trend mirrored in the HSCR chronic group though not reaching statistical significance (10.6 vs 19.07%, p=0.1195). For CO, the increase in caspase-3+ cells from 14.4 to 27.08% was significant (p=0.0101) in the chronic condition. However, such a difference was not evident in the acute group. Overall, HSCR and CO showed similar amounts of Caspase3+ cells before and after stimulation.

Necroptosis (RIPK3+/Caspase3-): The analysis revealed no significant differences in the detection of necroptotic cells neither between the HSCR and CO groups nor within their respective subgroups, as seen in Fig. 3vi. All significant results of this

section are summarized in Table 4Treatment resulted an in increase in RIPK1-independent apoptosis after acute stimulation in HSCR and chronic stimulation in CO, but not vice versa.

Table 3 Effects of Treatment on Apoptotic and Necroptotic Pathways in Zombie+ (Dead) Cells Across Chronic and Acute HSCR and CO Groups

Zombie Status	Analysis Group	Group	Measurement	Key Findings	*p*-value
dead (Zombie+)	chronic	HSCR	RIPK1-Apoptosis (RIP3+/Caspase3+)	↓ after treatment	0.0026
dead (Zombie+)	chronic	CO	RIPK1-Apoptosis (RIP3+/Caspase3+)	↓ after treatment	0.0407
dead (Zombie+)	acute	HSCR	Apoptosis (RIP3-/Caspase3+)	↑ after treatment	0.0220
dead (Zombie+)	chronic	HSCR	Apoptosis (RIP3-/Caspase3+)	↑ after treatment	0.0158
dead (Zombie+)	chronic	CO	Apoptosis (RIP3-/Caspase3+)	↑ after treatment	0.0159
dead (Zombie+)	acute	CO	Necroptosis (RIP3+/Caspase3-)	↓ after treatment	0.0182

Analysis reveals that RIPK1-dependent apoptosis is significantly reduced after chronic treatment, while increasing RIPK1-independent apoptotic processes at the same time. Still, RIPK1-dependent apoptosis was more prominent in chronic than in acute treated CO, but not in HSCR. RIPK1-independent apoptosis also increased after acute treatment in HSCR, but not in CO.

Table 4 Impact of Treatment on Apoptosis in Zombie− (Alive) Cells in Acute HSCR and Chronic CO Groups

Zombie Status	Analysis Group	Group	Measurement	Key Findings	*p*-value
alive (Zombie-)	acute	HSCR	Apoptosis (RIP3-/Caspase3+)	↑ after treatment	0.0474
alive (Zombie-)	chronic	CO	Apoptosis (RIP3-/Caspase3+)	↑ after treatment	0.0101

Treatment resulted an in increase in RIPK1-independent apoptosis after acute stimulation in HSCR and chronic stimulation in CO, but not vice versa.

Fig. 3

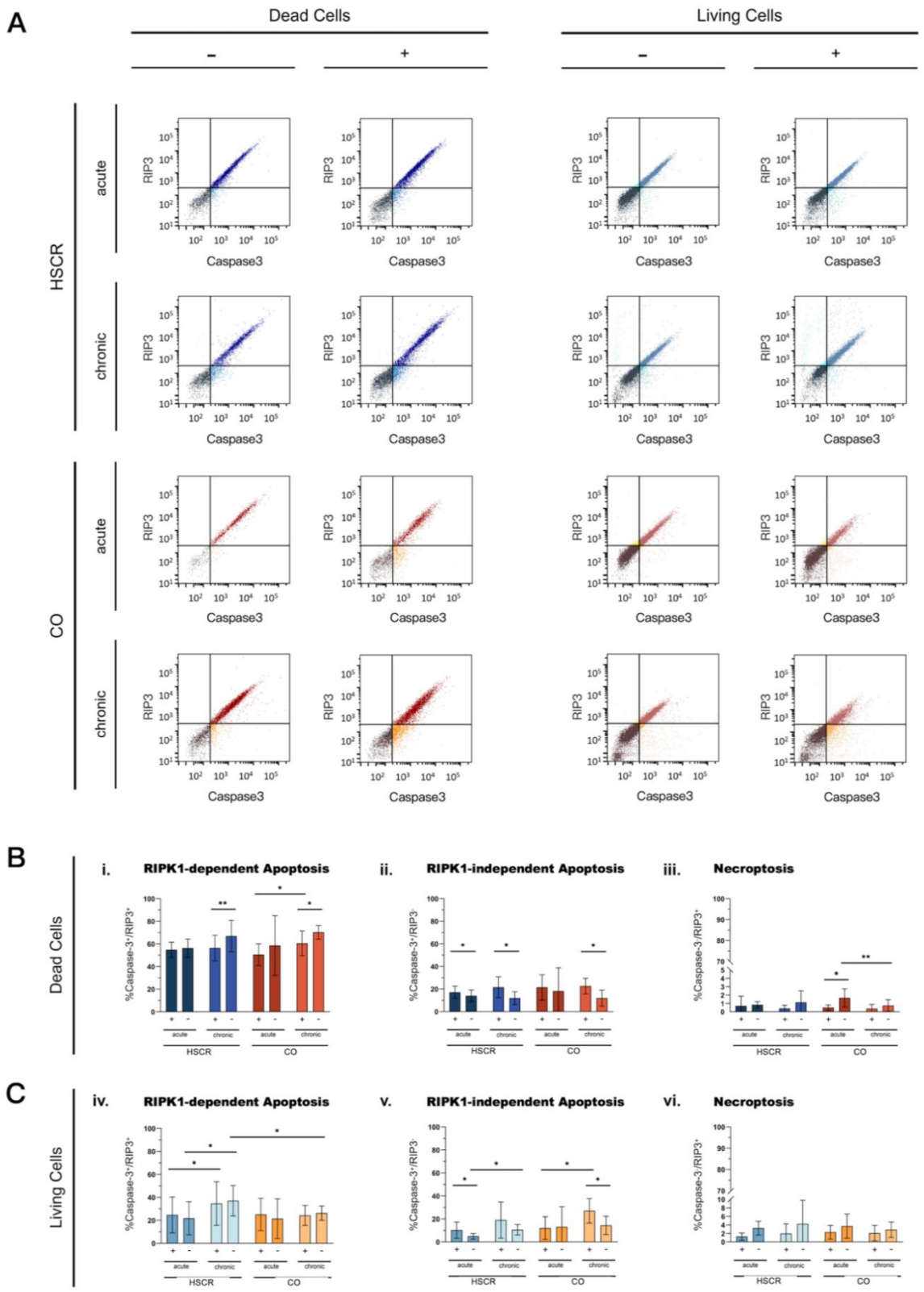

The percentages of Caspase3+/RIP3+ cells indicating RIPK1-dependent apoptosis, RIPK1-independent apoptosis, and necroptosis in dead and living cells under different conditions.

Panels (a) to (c) show data for dead cells, while panels (d) to (f) show data for living cells. The conditions compared include acute and chronic treatments, with and without the involvement of RIPK1, in HSCR and CO cells. Statistical significance is denoted by asterisks (*p<0.05, **p<0.01), indicating differences between the specified conditions. Error bars represent the standard deviation of the mean. Dead cells exhibit a reduction in RIPK1-dependent apoptosis following acute stimulation (a), whereas RIPK1-independent apoptosis rises across all treatment regimens (b). Necroptosis was minimally detectable and only showed notable changes in the CO groups (c). Among living cells, no significant differences in RIPK1-dependent apoptosis were observed within subgroups, but HSCR generally showed more living cells after chronic stimulation compared to acute stimulation (d). Similarly, RIPK1-independent apoptosis increased post-stimulation in most subgroups (e). Necroptosis had a minimal impact on living cells undergoing cell death (f).

1.3.4 Light microscopy of intestinal organoids

Under light microscopy, organoids from both HSCR patients and non-HSCR controls initially presented with well-defined crypt structures and complex morphology. After acute proinflammatory stimulation with TNF-α, IL-6, and IL-1β, HSCR organoids displayed a marked increase in cell death, characterized by structural disintegration and loss of structural integrity. Chronic stimulation led to further changes in the studied organoids, resulting in a rounded shape with thickened walls, suggesting a progressive loss of crypt structure complexity (Fig. 4).

Fig. 4

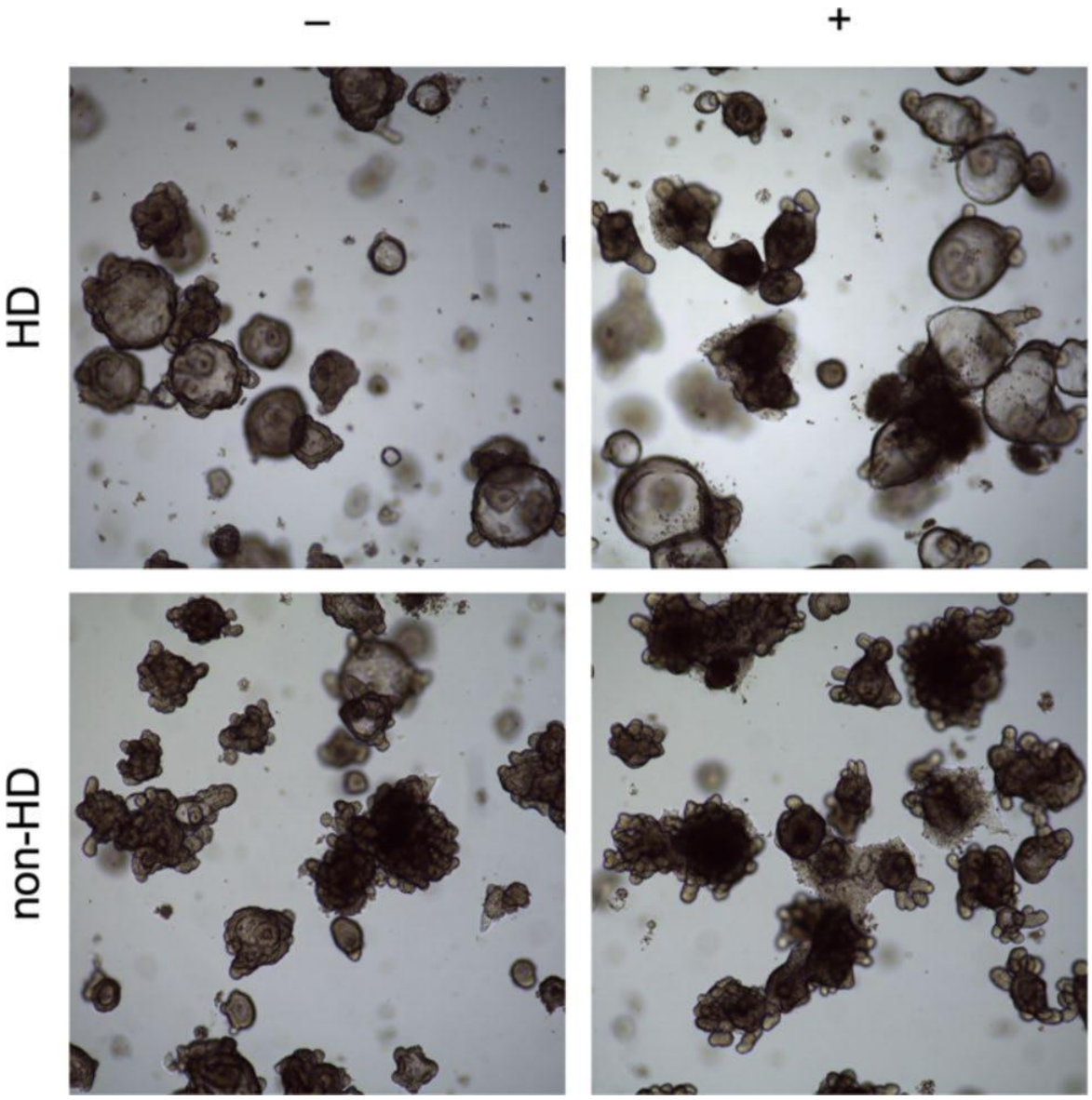

Light microscopy images of intestinal organoids from two patients, one suffering from Hirschsprung's disease (HSCR) and one serving as non-HSCR control, before and after acute proinflammatory treatment. Tissue specimens prepared from colon sections, ganglionic in case of HSCR. Mucosa preparation, organoid isolation, and culture treatment were performed as described. 4 × Magnification. Images taken with a Leica DM IL LED microscope. Acute proinflammatory stimulation results in increased cell death with disintegration of organoid structure and signs of cell death. Complexity of overall organoids morphology as seen before stimulation is mainly maintained.

1.3.5 Immunofluorescence staining of organoids and confocal microscopy analysis

Immunofluorescence staining with β-catenin and ZO-1 revealed a strong response to proinflammatory stimuli. Before stimulation, the studied organoids exhibited strong expression of β-catenin (red) and ZO-1 (green), indicating intact cell junctions and well-organized epithelial layers. Following acute proinflammatory treatment, organoids showed disrupted β-catenin and ZO-1 staining, with a diffuse and disorganized pattern suggestive of compromised cell junctions and increased permeability. DAPI staining

revealed fragmented nuclei, indicating apoptotic cell death. Confocal microscopy provided a detailed assessment of the alterations in organoid structure following proinflammatory stimulation. Acute treatment in HSCR organoids led to notable nuclear destruction, as evidenced by DAPI staining, and a loss of β-catenin and ZO-1 outlines, indicating compromised barrier function. Chronic stimulation exacerbated these effects. Z-stack imaging showed that in chronic conditions, the HSCR organoids lost much of their crypt architecture and appeared to have increased wall thickness, suggesting a reactive remodeling in response to sustained inflammatory stress (Fig. 5).

Fig. 5

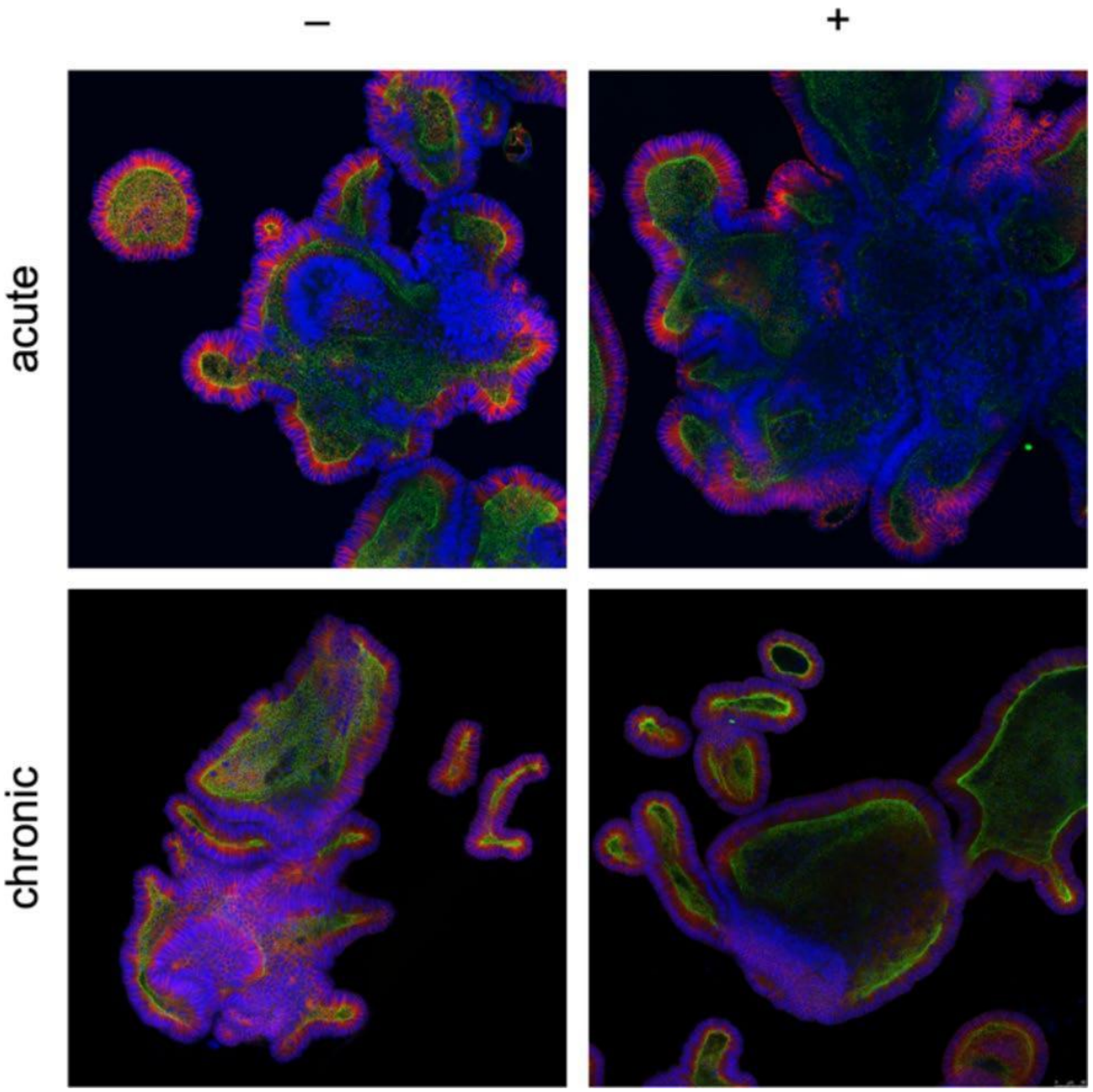

Immunofluorescence microscopy of intestinal organoids from a patient with Morbus Hirschsprung. Outlining of the organoids marked by intestinal barrier markers beta-catenin (red) and ZO-1 (green), nuclei stained with DAPI (blue) for orientation. 20 × Magnification, images taken with the Olympus FV 3000 (acute) and Leica SP5 (chronic) confocal microscopes. Before stimulation, enter-oids present with defined crypt structures and complex morphology. Acute treatment with proinflammatory cytokines leads to increased cell death, seen by nuclei destruction and loss of outlines. Following chronic treatment, organoids lost most of the crypt structure complexity and presented round with thickened wall diameter.

1.4 Discussion

The introduction of this assay into spheroid cultures marks a significant advancement in the study of cell death, providing a nuanced understanding of apoptosis and revealing the role of RIPK1 in non-viable cells. By enabling a detailed examination of cell death phenotypes in both viable and non-viable populations, this approach enables for the identification of classic apoptosis through Caspase3 positivity and the elucidation of RIPK1-mediated mechanisms (Lee et al. 2018). Utilizing a proinflammatory cocktail of TNF-α, IL-6, and IL-1β to mimic the inflammatory environment of inflammatory bowel disease (IBD), we observed clear differences in the cellular responses to acute versus chronic inflammation (d'Aldebert et al. 2020). Light microscopy (Fig. 4) and immunofluorescence (Fig. 5) of intestinal organoids derived from patients with Hirschsprung's disease (HSCR) demonstrated profound structural alterations under proinflammatory conditions. Initially, the organoids exhibited well-defined crypt structures and complex morphology. However, acute proinflammatory stimulation led to a marked increase in cell death, indicated by nuclear destruction and a loss of cellular outlines. Chronic stimulation exacerbated this effect, resulting in a significant reduction in structural complexity, with organoids becoming rounded and developing thicker walls. HSCR organoids displayed considerable disintegration and cell death. These indicate that HSCR organoids have a unique and compromised response to inflammatory stress, highlighting an altered epithelial barrier and immune function in the disease. This work not only underscores the vulnerability of HSCR tissues to inflammatory stimuli but also emphasizes the critical role of inflammatory pathways in the pathophysiology of HSCR.

Under acute conditions, HSCR specimens exhibited an increased number of dead cells (Zombie+) compared to chronic stimulation, a pattern also seen in control specimens. This suggests an adaptive cellular response over time, transitioning toward survival mechanisms. Additionally, although not statistically significant, HSCR tissues had more dead cells than controls, indicating distinct responses to inflammatory challenges in HSCR.

Distinguishing between RIPK1-independent and RIPK1-dependent apoptosis is crucial due to their differing biological implications (Gunther et al. 2013). RIPK1-independent apoptosis is typically immunologically silent, avoiding an inflammatory response. In contrast, RIPK1 functions as both a kinase and scaffold, balancing cellular survival, apoptosis, and necroptosis(Kondylis et al. 2017, Wong et al. 2020).

Its activation can shift cellular fate toward inflammatory pathways, especially when influenced by proinflammatory cytokines such as TNF-α, IL-6, and IL-1β (van Loo and Bertrand 2023). Clinically, aberrant RIPK1 signaling is associated with inflammatory conditions such as IBD, where it regulates the transition of NF-κB signaling from cell survival to apoptosis or necroptosis(Kondylis et al., 2017, Wong et al. 2020). This dysregulation disrupts the intestinal barrier, allowing bacterial invasion and leading to enterocolitis. Given the histological similarity between IBD (particularly ulcerative colitis) and HAEC, it is plausible that aberrant RIPK1 signaling also contributes to HAEC pathogenesis (Austin 2012, Vlantis et al. 2016).

In the context of HSCR and HAEC, altered apoptotic pathways may explain the differential responses to inflammatory stimuli. Our study shows that in HSCR, cells are more inclined towards RIPK1-dependent apoptosis, which can link to proinflammatory signaling. This contrasts with the cellular environment in healthy controls, where apoptosis occurs in a more RIPK1-independent manner, often avoiding inflammatory escalation (Lu et al. 2020). Furthermore, serum-derived exosome microRNA-18a-5p has been shown to promote apoptosis in HAEC through the suppression of RORA and regulation of the SIRT1/NF-κB pathway, creating a proinflammatory microenvironment (Chen et al. 2021). Additionally, disruptions in neuroimmune regulation have been observed, suggesting a complex interplay between nerve cells and immune cells in HAEC, which could further drive the unique apoptotic landscape in these patients (Ji et al. 2023). This evidence underscores that in HSCR, apoptosis and its regulation via RIPK1 may play a more prominent role in the pathogenesis of HAEC, diverging significantly from the mechanisms observed in healthy controls. Understanding the dynamics between viable and nonviable cells is crucial, especially in how a proinflammatory stimulus can activate different cell death pathways within the same cell. A viable cell, despite initiating cell death processes, may initially balance these mechanisms depending on factors like RIPK1 availability. Over time, this balance shifts toward non-viability, progressing through apoptosis or necroptosis. Our analysis showed that viable cells in the HSCR group more frequently underwent RIPK1-dependent apoptosis, especially under chronic stress, whereas control group cells showed no difference between acute and chronic conditions. This may indicated a cellular trend in HSCR toward classic apoptosis when RIPK1 becomes less available over time upon proinflammatory stimulation (Table 3, Fig. 3v). In non-viable cells, a more pronounced regulatory role for RIPK1 was observed, as evidenced by a decrease in

RIPK1-dependent apoptosis upon chronic stimulation. This adaptive modulation in apoptotic pathways indicates that cells, under prolonged stress, may recalibrate their mechanisms to avoid the inflammatory pathways initially triggered by RIPK1(Pasparakis and Vandenabeele 2015). This shift could represent an attempt by the tissue to adapt to sustained damage or a progression toward a more critical pathological state(Newton et al. 2014).The low presence of necroptotic cells (RIPK3 + /Caspase3−) across both HSCR and control groups further emphasizes that necroptosis, a highly proinflammatory cell death process, plays a subordinate role in this experimental context (Fig. 3C vi). While necroptosis, characterized by cell membrane rupture and pro-inflammatory signaling (Gunther et al. 2013), appeared to have a minimal impact on cell death in our model, this finding should be interpreted with caution It remains unclear whether this reflects a true biological absence of necroptotic activity under the conditions tested, or whether it is a limitation of the marker system and detection sensitivity employed in this study. Further investigation using complementary approaches may be necessary to fully assess the role of necroptosis in HSCR pathology.

One major limitation of this study is the small sample size, with only five HSCR and five control patients included. While this is within acceptable limits for organoid-based investigations, it may limit the generalizability and statistical power of the findings. Larger cohorts will be required to validate and extend these observations.

Future studies should validate these findings in animal models of HSCR or HAEC and assess whether pharmacological modulation of RIPK1 alters disease susceptibility. Additionally, single-cell RNA-sequencing of organoids under inflammatory stress may refine our understanding of epithelial heterogeneity in cell death susceptibility.

1.5 Conclusions

In this study, we developed and applied a novel flow cytometry-based assay to analyze programmed cell death subtypes in colonic organoids from HSCR patients and controls. Our findings demonstrate that HSCR organoids display a distinct susceptibility to acute and chronic inflammatory stimuli, with a marked shift in apoptosis signaling pathways.

Under acute inflammation, HSCR cells showed increased overall cell death, especially in the RIPK1-dependent subpopulation. In contrast, chronic stimulation favored RIPK1-independent apoptosis, suggesting adaptive modulation of epithelial cell death mechanisms.

These results highlight the central role of RIPK1 in regulating epithelial cell fate under inflammatory conditions in HSCR, offering a mechanistic explanation for the vulnerability of HSCR patients to HAEC and a rationale for RIPK1-targeted therapeutic strategies.

2. Artikel oder Manuskript mit Letter of Acceptanc

Subject [EXT] Pediatric Surgery International - Receipt of Manuscript 'Dissecting the dynamics...'
From Pediatric Surgery International <moses.kanagadass@springernature.com>
To <zhongwen.li@stud.uke.uni-hamburg.de>
Date 2024-10-07 11:46

Ref: Submission ID 80d9920e-2dae-4f22-8035-1e6155e86e0e

Dear Dr Li,

Please note that you are listed as a co-author on the manuscript "Dissecting the dynamics of cell death pathways in Hirschsprung's Disease: A comparative analysis of viable and non-viable cells under proinflammatory conditions", which was submitted to Pediatric Surgery International on 07 October 2024 UTC.

If you have any queries related to this manuscript please contact the corresponding author, who is solely responsible for communicating with the journal.

Kind regards,

Editorial Assistant
Pediatric Surgery International

Pediatric Surgery International (2024) 40:288
https://doi.org/10.1007/s00383-024-05862-2

ORIGINAL ARTICLE

Dissecting the dynamics of cell death pathways in Hirschsprung's disease: a comparative analysis of viable and non-viable cells under proinflammatory conditions

Zhongwen Li[1] · Johanna Hagens[1] · Clara Philippi[1] · Hans Christian Schmidt[1] · Lucie Rohwäder[1] · Pauline Schuppert[1] · Laia Pagerols Raluy[1] · Magdalena Trochimiuk[1] · Konrad Reinshagen[1] · Christian Tomuschat[1]

Accepted: 16 October 2024 / Published online: 3 November 2024

Abstract

Purpose The present study explores the dynamics of cell death in Hirschsprung's disease (HSCR) and control (CO) groups under inflammatory stress conditions.

Methods Using flow cytometry, we analyzed intestinal colonic organoid cultures derived from the ganglionic segment of the HSCR and CO groups. Our analysis focused on the quantification of RIPK1-independent and RIPK1-dependent apoptosis, as well as necroptosis in both viable and non-viable cells under acute and chronic inflammatory stress.

Results Our findings indicate that HSCR cells are particularly vulnerable to inflammation during acute proinflammatory stress, as evidenced by an increase in dead cells (Zombie +). Under chronic conditions, adaptive changes are observed in both HSCR and CO groups, indicating survival mechanisms. These adaptations are uniquely altered in HSCR, suggesting an impaired response to chronic inflammation. HSCR cells show significantly decreased RIPK1-dependent apoptosis in acute scenarios compared to chronic ones, unlike the CO group, implying varied responses to different inflammatory stresses. In non-viable cells, considerable changes in RIPK1-dependent apoptosis under chronic conditions in HSCR indicate a heightened inflammatory response compared to CO.

Conclusion This research provides insights into cell death regulation in HSCR under inflammatory stress by using patient-derived organoids, underscoring the complexity of its inflammatory response.

Keywords Organoids · RIK1 · RIP3–caspase-3 assay · Hirschsprung's disease · Apoptosis · Necroptosis

Abbreviations

CO	Control group
FSC-A	Forward scatter area
HAEC	Hirschsprung-associated enterocolitis
HSCR	Hirschsprung's disease
IBD	Inflammatory bowel disease
IL-1β	Interleukin 1 beta
IL-6	Interleukin 6
ODM-h	Organoid differentiation medium human
OGM-h	Organoid growth medium human
RIPK1	Receptor-interacting protein kinase 1
RIPK3	Receptor-interacting protein kinase 3
SSC-A	Side scatter area
TNFR1	Tumor necrosis factor receptor 1
TNF-α	Tumor necrosis factor alpha

Zhongwen Li and Johanna Hagens contributed equally to this work.

✉ Christian Tomuschat
c.tomuschat@uke.de

[1] Department of Pediatric Surgery, University Medical Center Hamburg-Eppendorf, Hamburg, Germany

Introduction

Hirschsprung disease (HSCR) is a congenital disorder characterized by a lack of ganglion cells in the enteric nervous system, affecting approximately one in 5,000 live births [1]. This condition leads to considerable gastrointestinal problems due to neuroblasts failing to migrate during embryonic development, resulting in various clinical symptoms based on the extent of intestinal involvement [2]. The primary treatment involves surgically removing the aganglionic section. Nonetheless, genetic factors, especially mutations in genes like the Ret proto-oncogene (RET) and endothelin receptor type B (EDNRB), add complexity to HSCR's origins [3]. Additionally, HSCR patients are susceptible

to Hirschsprung-associated enterocolitis (HAEC) [4–6]. Moreover, recent epidemiological studies have reported an increased incidence of inflammatory bowel disease (IBD) among HSCR patients [4, 6–8]. These recent studies raise questions such as: Could there be a shared pathophysiology between HSCR, HAEC, and IBD? Do the similarities in apoptotic and necroptotic pathways point to common underlying mechanisms? Are the treatment responses in HSCR and CO cells indicative of broader disease progression connections?

At the molecular level, the receptor interacting protein kinase (RIPK) family, particularly RIPK1 and RIPK3, appears to be a promising target. These kinases are crucial for maintaining intestinal barrier integrity and regulating cell death mechanisms. The signaling pathways mediated by RIPKs, which shift from cell survival to apoptotic (RIPK1-dependent) or necroptotic cell death (RIPK3-dependent), may present a connection since dysregulation of these pathways has been documented in IBD [9].

Using flow cytometry and directly conjugated monoclonal antibodies, we analyzed cell death pathways in patient-derived organoid cultures from HSCR patients and controls. To achieve this, we refined an assay to measure various pathways using FACS in organoid cultures [10].

This method enabled us to differentiate between cell death mechanisms within cell populations derived from colonic organoids. Consequently, we identified previously unnoticed, yet significant small and large cell groups undergoing various stages of RIPK1-dependent apoptosis (RIPK1 +), RIPK1-independent apoptosis (Caspase-3 +), and necroptosis (RIPK3 +), in both viable and non-viable cells. Determining whether cells are viable (Zombie −) or non-viable (Zombie +) and their respective cell death pathways is critical for diagnosing diseases and understanding their progression. For example, in gastrointestinal diseases, the balance between viable and non-viable epithelial cells significantly affects the intestinal barrier's integrity [11]. In this study, we observed that a proinflammatory cocktail containing TNF-α, IL-6, and IL-1β can simultaneously induce multiple forms of cell death within a single cell [12]. We demonstrated activated pathways exhibiting high levels of RIPK1-dependent apoptosis, RIPK1-independent apoptosis, and necroptosis [13].

Materials and methods

Establishment and maintenance of organoids

The study adhered to the Declaration of Helsinki guidelines and received approval from the Institutional Review Board Hamburg ethics committee (PV5251). Tissues from patients with Hirschsprung's disease (HSCR, $n = 5$) were sourced from surgically removed specimens, exclusively using the proximal ganglionic portion. Control tissues (CO, $n = 5$) were obtained from patients undergoing surgeries unrelated to Hirschsprung's disease, ensuring a balanced comparison (Table 1). The samples were immediately placed in Iscove's modified Dulbecco's medium (IMDM, #12440053, Gibco Thermo Fisher Scientific, Waltham, MA, USA), supplemented with 20% fetal bovine serum (FBS, #0500-064, Thermo Fisher Scientific, Waltham, MA, USA) and 1% penicillin/streptomycin (P/S, #PS/B, Capricorn Scientific, Ebsdorfergrund, Germany). Afterward, they were thoroughly washed with sterile Dulbecco's phosphate-buffered saline (DPBS; #37350, Gibco Thermo Fisher Scientific, USA), and the mucosal layer was carefully separated from underlying tissues, then cut into 1–2 mm pieces. Mucosal cells were isolated by incubating tissue slices in IMDM with 5 mM ethylenediaminetetraacetic acid (#15575–038, Invitrogen,

Table 1 Patient characterristics for each sample used in this study

Sample	Gender	Age at operation (months)	Trisomy status	Diagnoses	Median group age
#1	Male	3.6	Negative	Hirschsprung's disease	14.4
#2	Male	3.8	Positive	Hirschsprung's disease, atrial septum defect, persistent oval foramen	
#3	Female	16.9	Negative	Hirschsprung's disease	
#4	Female	14.4	Negative	Hirschsprung's disease	
#5	Female	14.5	Negative	Hirschsprung's disease	
#6	Female	6.2	Negative	Anal atresia, persistent oval foramen, kidney dysplasia, clubfoot	7.3
#7	Female	9.3	Negative	anal atresia, atrial septum defect, kidney dysplasia, hemivertebrae, multiple ribs, sacral dysplasia, heel feet	
#8	Male	7.3	Negative	anal atresia, hypospadia sine hypospadia	
#9	Male	4.9	Negative	ileo-colic invagination	
#10	Male	12.8	Negative	anal atresia, esophageal atresia, ventricular septum defect, fused kidneys, sacral agenesia	

Waltham, MA, USA) and 2 mM DL-dithiothreitol (DTT, #D9779-5G, Sigma-Aldrich, St. Louis, MO, USA) for 20 min at 4 °C, facilitating crypt structure isolation. They were further filtered through a 70 µm cell strainer (#352350, Corning, Corning, NY, USA) and washed in IMDM containing 2% FBS and 1% P/S, as well as Advanced Dulbecco's modified Eagle medium (Advanced DMEM, #12491-015, Gibco Thermo Fisher Scientific, USA), which includes 1% 4-(2-hydroxyethyl)-1-piperazineethanesulfonic acid (HEPES, #H3537-100ML, Sigma-Aldrich, St. Louis, MO, USA), 1% GlutaMAX (#35050-061, Gibco Thermo Fisher Scientific, Waltham, MA, USA), and 1% P/S, collectively referred to as 'Adv.+++'. Each washing step was followed by centrifugation at 500×*g* and 4 °C for 10 min. A solution consisting of extracellular matrix in a 1:2 ratio (Cultrex UltiMatrix, #BME001, R and D Systems, Minneapolis, MN, USA) was prepared. The suspension was pipetted as 30 µl droplets into the center of each well in a 24-well plate (#3022521, Sarstedt AG and for 30 min to solidify the Cultrex. Subsequently, each well received 500 µl of Organoid Growth Medium Human (OGM-h, #060610, Stemcell Technologies, Canada), enriched with 5 mM ROCK-Pathway Inhibitor (ROC, #72302, Stemcell Technologies, Vancouver, Canada), 1% penicillin/streptomycin (P/S), and 0.02% Primocin (#ant-pm-05, InvivoGen, San Diego, CA, USA), with medium changed every 2–3 days.

After 7–10 days, organoids achieved the necessary confluence for passage. For dissociation, the Cultrex dome was mechanically disrupted in Adv.+++, and the cell suspension was centrifuged at 300×*g* and 4 °C for 5 min. Organoids were further broken down by pipetting 30–50 times. Following centrifugation for cell isolation and supernatant removal, cells were resuspended in Adv.+++and embedded once again using Cultrex following the previously described protocol. Organoids were maintained in OGM-h containing 1% P/S, with the medium replaced every 2–3 days. Daily evaluations were conducted to monitor structural development and ensure their readiness for experimental use.

Preparation of organoids for flow cytometry

Organoids were assigned to two different experimental conditions: acute and chronic treatment groups (Fig. 1). Within each group, samples were further divided into untreated and treated subsets. The treated subsets received a cytokine cocktail containing TNF-α (#300-01A, PeproTech, London, UK), IL-6 (#200-06, PeproTech, London, UK), and IL-1β (#200-01B, PeproTech, London, UK) at a concentration of 10 ng/ml for each cytokine, as determined by preliminary experiments [12]. All organoids were cultured in OGM-h until day 5. Thereafter, differentiation was induced by switching the medium to Organoid Differentiation Medium Human (ODM-h, #100-02114, Stemcell Technologies, Vancouver, Canada) with 1% P/S. In the chronic treatment protocol, treated organoids received the cytokine cocktail on days 3 and 5. In contrast, the acute treatment protocol involved administering the cytokine cocktail on days 5, 6, and 7. Untreated subgroups under both chronic and acute conditions received no cytokine cocktail.

For flow cytometry analysis, organoids were detached from Cultrex domes and resuspended in Adv.+++. After centrifugation at 300×g and 4 °C for 5 min, organoids were broken down into single cells using TrypLE (#12,605,028, Gibco Thermo Fisher Scientific, Waltham, MA, USA) at 37 °C for 4 min. Following incubation, cells were washed with Adv.+++and centrifuged again at 300×g and 4 °C for 5 min. The supernatant was discarded, and cell pellets were stained with Zombie NIR fluorescent dye (#423105, BioLegend, San Diego, CA, USA, dilution 1:2000) in DPBS for 30 min at 4 °C in the dark. Cells were then washed in DPBS and fixed using eBioFix intracellular fixation buffer (#00-8222-49, BD Biosciences, San Jose, CA, USA) for 20 min at 4 °C. Subsequently, cells were permeabilized with 0.25% Triton X-100 (#T8787, Sigma-Aldrich, St. Louis, MO, USA) for 15 min at 4 °C in darkness. Finally, cells were labeled with anti-RIPK3-Alexa Fluor 488 (clone B-2, #sc-374639AF488, Santa Cruz Biotechnology, Dallas, TX, USA, dilution 1:125) and anti-active caspase-3–BV650

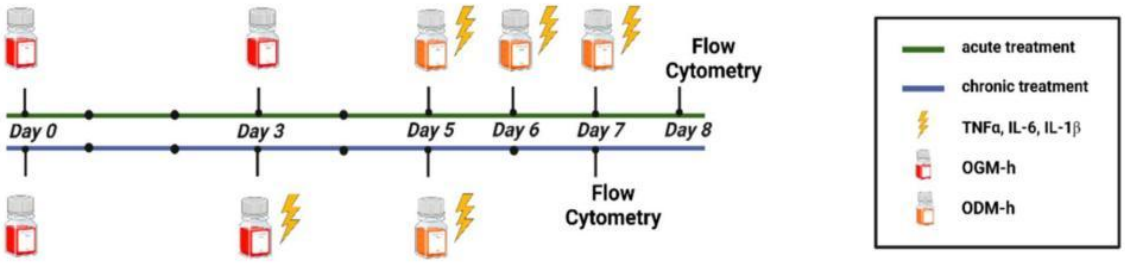

Fig. 1 Experimental setup. Enteroids from both CO and HSCR were maintained in standard growth medium for 5 days and then differentiated until flow cytometry took place. Proinflammatory stimulation was achieved through a cytokine combination of TNFα, IL-1β, and IL-6 at days 3 and 5 for chronic and days 5, 6, and 7 for the acute regimen. Figure created with BioRender.com

(clone C92-605, #564096, BD Biosciences, San Jose, CA, USA, dilution 1:50) for 20 min at 4 °C in the dark.

RIPK3–caspase-3 analysis using flow cytometry

Flow cytometric analysis was performed on 10,000 individual cells from each subgroup using the BD LSRFortessaTM (BD Biosciences, San Jose, CA, USA). Zombie NIR dye detection was facilitated by a 633 nm laser, with signal collection at 780/60 nm. Caspase-3–BV650 fluorescence was identified using a 405 nm laser and collected at 675/30 nm. RIPK3–Alexa Fluor 488 fluorescence was captured by a 488 nm laser and collected at 585/40 nm. Cell debris was excluded by gating based on forward scatter-area (FSC-A) versus side scatter-area (SSC-A) dot plots. Cells were further analyzed on a Zombie NIR versus SSC-A dot plot; all Zombie NIR-positive cells were considered dead. In contrast, Zombie NIR-negative cells, assumed to be viable, were gated on an FSC-A versus SSC-A plot. A more precise distinction between living and dead cells was achieved using caspase-3–BV650 versus RIPK3–Alexa Fluor 488 dot plots. Cells expressing caspase-3 alone were categorized as undergoing classic (RIPK1-independent) apoptosis, while those positive for only RIPK3 were classified as undergoing necroptosis. Cells positive for both caspase-3 and RIPK3 were interpreted as experiencing RIPK1-dependent apoptosis. Zombie + cells negative for both markers were presumed to follow an alternative cell death pathway. Fluorescence minus one (FMO) control was utilized for cell identification, gating, and color compensation. Data were analyzed using FlowLogic software version 8.7 (Inivai Technologies, Victoria, Australia).

Light microscopy

Organoids were imaged using a Leica DM IL LED microscope at 4 × magnification. Images were taken directly in their culture wells without fixation or staining to preserve the native structure. Organoids were photographed before and after proinflammatory stimulation at specified time points to observe morphological changes, including crypt structure integrity and signs of cell death. Image analysis was conducted using ImageJ to evaluate structural alterations and overall morphology of the organoids.

Immunofluorescence staining and confocal microscopy

Organoids were fixed in 4% paraformaldehyde, permeabilized with 0.5% Triton X-100, and blocked with 5% BSA to reduce non-specific antibody binding. They were then incubated with primary antibodies against β-catenin (1:200) and ZO-1 (1:200) overnight at 4 °C, followed by incubation with Alexa Fluor-conjugated secondary antibodies (1:500) for 1 h. DAPI (1 µg/mL) was used to stain nuclei. Confocal images were acquired using an Olympus FV 3000 for acute treatment and a Leica SP5 for chronic treatment, at 20 × magnification. Z-stack images provided detailed views of the organoid structure, highlighting the localization of β-catenin (red) and ZO-1 (green), with DAPI marking nuclei (blue). Image analysis was performed using ImageJ to assess changes in cellular morphology and junction integrity.

Statistical analysis

Statistical analyses were conducted with GraphPad Prism version 10.1 (GraphPad Software, San Diego, CA, USA). Subgroup analysis employed the paired t test, while mean values and standard deviations (SD) were computed for each dataset. A p value less than 0.05 was considered to indicate statistical significance.

Results

Acute proinflammatory treatment causes increased cell death

The analysis distinguished between non-viable and viable cells by their Zombie-status. Figure 2 shows a significant difference in the proportion of Zombie-positive cells

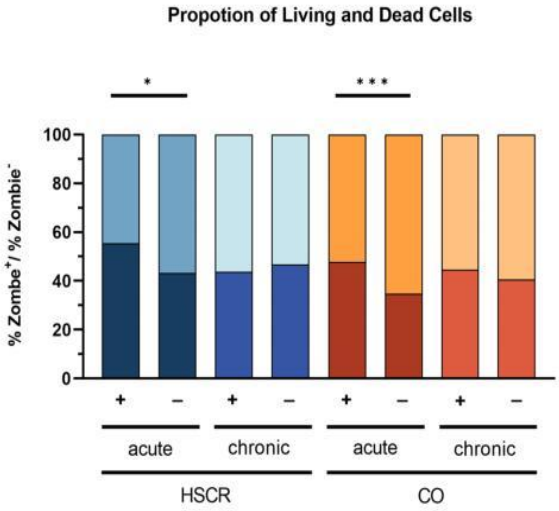

Fig. 2 Proportions of dead and living cells. Analysis includes five enteroids for each measured subgroup. Cell proportions are shown for acute and chronic stimulation scheme before (–) and after treatment (+). Whole cell population was separated according to their zombie status. Zombie$^+$ cells were marked as dead. Zombie – cells were marked as alive and undergoing cell death. Analysis reveals a significant increase in dead cells after acute proinflammatory stimulation for both HSCR ($p = 0.0029$) and CO ($p = 0.0009$)

between treated and untreated subgroups during acute stress. In the HSCR acute group, Zombie + cells were significantly increased in the treated subgroup (55.39 vs. 43.33%, $p = 0.0229$). Similarly, in the control acute group, treated subgroups had more Zombie + cells than untreated ones (47.71 vs. 34.70%, $p = 0.009$). However, under chronic stress, both HSCR and control groups showed a considerable number of dead cells before and after treatment, with no significant differences (Table 2).

Death cells undergo RIPK1-independent apoptosis after proinflammatory stimulation

RIPK1-dependent apoptosis (RIPK3 + /caspase-3 +): was observed as the main cell death mechanism in non-viable cells, as depicted in Fig. 3i. After acute treatment, HSCR organoids exhibited similar levels of double-positive cells (54.88 vs. 56.30%, $p = 0.2825$), while chronic stimulation resulted in a notable decrease in double positivity (66.95 vs. 56.42%, $p = 0.0026$). Similarly, CO organoids under chronic treatment showed a significant drop in double-positive cells (70.35 vs. 60.55%, $p = 0.0407$); however, acute treatment did not demonstrate significant changes, with RIPK3 + /caspase-3 + cells decreasing from 58.59 to 50.50% ($p = 0.2094$).

RIPK1-independent apoptosis (RIPK3$^-$/caspase-3$^+$). HSCR samples showed a significant increase in RIPK1-independent apoptosis after stimulation for both acute and chronic treatment (14.09 vs. 17.11%, $p = 0.0220$; 12.01 vs. 21.61%, $p = 0.0158$, respectively). While CO cells also presented with this pattern for chronic treatment, increasing from 11.93 to 22.59% ($p = 0.0159$), acute stimulation showed no affection (18.24 vs. 21.53%, $p = 0.3140$). HSCR and CO showed similar rates in caspase-3$^+$ cells before and after treatment, as summarized in Fig. 3ii.

Necroptosis (RIPK3$^+$/caspase-3$^-$). Overall, necroptosis was just slightly detectable and showed no significance in HSCR cell death in both treatment regimens (Fig. 3iii). While chronic CO samples appeared similar, acute treatment of controls demonstrated a decline in necroptotic cells post-treatment from 1.66 to 0.50% ($p = 0.0182$).

The significant results of all the dead cell analysis are summarized in Table 3.

Analysis reveals that RIPK1-dependent apoptosis is significantly reduced after chronic treatment, while increasing RIPK1-independent apoptotic processes at the same time. Still, RIPK1-dependent apoptosis was more prominent in chronic than in acute treated CO, but not in HSCR. RIPK1-independent apoptosis also increased after acute treatment in HSCR, but not in CO.

Living cells undergo RIPK1-dependent apoptosis after proinflammatory stimulation

RIPK1-dependent apoptosis (RIPK3$^+$/caspase-3$^+$). RIPK1-dependent apoptosis remained the leading cause of cell death in still viable cells, but subgroup analysis was not able to detect significant changes for pre- and posttreatment, as summarized in Fig. 3iv. Following acute treatment, HSCR organoids showed slight decline after treatment (24.69 vs. 21.89%, $p = 0.4065$), and chronic stimulation led to a slight rise (34.67 vs. 37.12%, $p = 0.7339$). This was also observed for acute and chronic treated CO organoids (25.14 vs. 21.46%, $p = 0.6885$; 24.29 vs. 26.25%, $p = 0.5594$).

RIPK1-independent apoptosis (RIPK3$^-$/caspase-3$^+$). As shown in Fig. 3v, there was a marked increase in cells undergoing apoptosis in the HSCR acute treated group, ranging from 4.93 to 10.35% ($p = 0.0474$), a trend mirrored in the HSCR chronic group though not reaching statistical significance (10.6 vs. 19.07%, $p = 0.1195$). For CO, the increase in caspase-3$^+$ cells from 14.4 to 27.08% was significant ($p = 0.0101$) in the chronic condition. However, such a difference was not evident in the acute group. Overall, HSCR and CO showed similar amounts of caspase-3$^+$ cells before and after stimulation.

Necroptosis (RIPK3$^+$/caspase-3$^-$). The analysis revealed no significant differences in the detection of necroptotic cells neither between the HSCR and CO groups nor within their respective subgroups, as seen in Fig. 3vi. All significant results of this section are summarized in Table 4

Treatment resulted an in increase in RIPK1-independent apoptosis after acute stimulation in HSCR and chronic stimulation in CO, but not vice versa.

Light microscopy of intestinal organoids

Under light microscopy, organoids from both HSCR patients and non-HSCR controls initially presented with well-defined crypt structures and complex morphology. After acute proinflammatory stimulation with TNF-α, IL-6, and IL-1β, HSCR organoids displayed a marked increase in cell death,

Table 2 Summary of key findings on the effect of treatment on Zombie + (dead) cells in the acute HSCR and CO groups

Group	Zombie stain	Analysis group	Measurement	Key findings	*p* value
HSCR	Dead (Zombie$^+$)	Acute	% dead cells	↑After treatment	0.0029
CO	Dead (Zombie$^+$)	Acute	% dead cells	↑After treatment	0.009

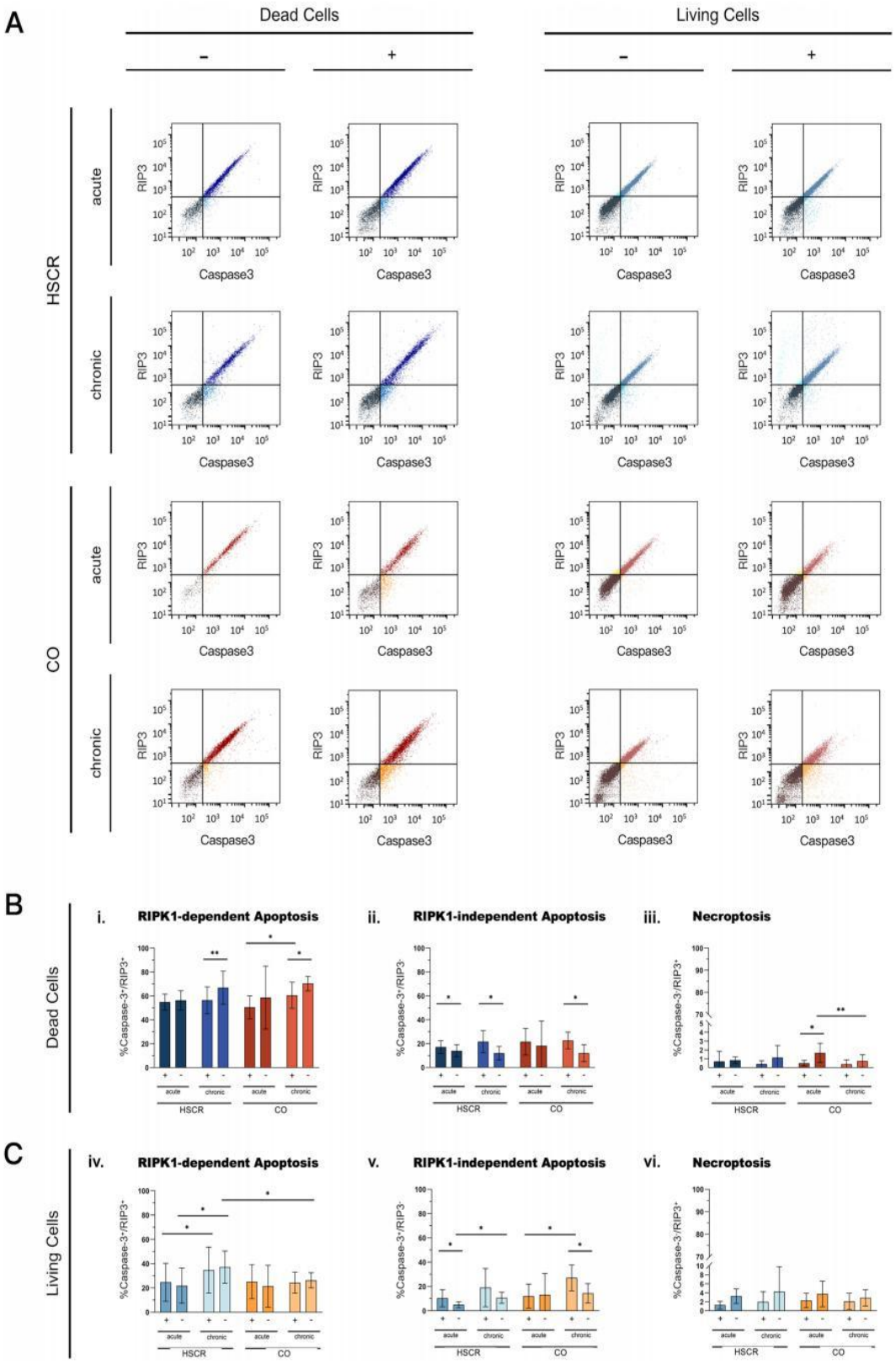
A
Dead Cells
Living Cells
-
+
HSCR
CO
acute
chronic
RIP3
Caspase3
B
Dead Cells
i. RIPK1-dependent Apoptosis
ii. RIPK1-independent Apoptosis
iii. Necroptosis
%Caspase-3+/RIP3+
%Caspase-3/RIP3+
HSCR
CO
C
Living Cells
iv. RIPK1-dependent Apoptosis
v. RIPK1-independent Apoptosis
vi. Necroptosis

◂**Fig. 3** Summary of FACS results. A RIP3 versus caspase-3 dot plots for two exemplary samples from HSCR and CO with gating of RIP3-positive (upper left), caspase-3 positive (lower right), double-positive (upper right) and double-negative (lower left) cells. Analysis was performed for dead (left column) and living (right column) cell populations. Dot plots depict the changes in subgroup populations after treatment with either acute (upper row) or chronic (lower row) cytokine cocktail. B Dead cells show a decrease in RIPK1-dependent apoptosis after acute and chronic stimulation (**i**), while RIPK1-independent apoptosis increases after all treatment regimens (**ii**). Necroptosis was barely detectable and only showed significant changes for the CO groups (**iii**). C Living cells presented no significant changes for RIPK1-dependent apoptosis within the subgroups, but HSCR overall showed more living cells following chronic compared to acute stimulated subgroups (**iv**). Again, RIPK1-independent apoptosis increased after stimulation for most subgroups (**v**). Necroptosis played only a minor role in living cells undergoing cell death (**vi**)

characterized by visible disintegration and loss of structural integrity. Chronic stimulation led to further changes in the studied organoids, resulting in a rounded shape with thickened walls, suggesting a progressive loss of crypt structure complexity (Fig. 4).

Immunofluorescence staining of organoids and confocal microscopy analysis

Immunofluorescence staining with β-catenin and ZO-1 revealed a strong respond toward proinflammatory inflammation. Before stimulation, the studied organoids exhibited strong expression of β-catenin (red) and ZO-1 (green), indicating intact cell junctions and well-organized epithelial layers. Following acute proinflammatory treatment, organoids showed disrupted β-catenin and ZO-1 staining, with a diffuse and disorganized pattern suggestive of compromised cell junctions and increased permeability. DAPI staining revealed fragmented nuclei, indicating apoptotic cell death. Confocal microscopy provided a detailed assessment of the alterations in organoid structure following proinflammatory stimulation. Acute treatment in HSCR organoids led to notable nuclear destruction, as evidenced by DAPI staining, and a loss of β-catenin and ZO-1 outlines, indicating compromised barrier function. Chronic stimulation exacerbated these effects. Z-stack imaging showed that in chronic conditions, the HSCR organoids lost much of their crypt architecture and appeared to have increased wall thickness, suggesting a reactive remodeling in response to sustained inflammatory stress (Fig. 5).

Discussion

The introduction of this assay into spheroid cultures marks a significant advancement in the study of cell death, providing a nuanced understanding of apoptosis and revealing the role of RIPK1 in non-viable cells. By enabling a detailed examination of cell death phenotypes in both viable and non-viable populations, this technique allows for the identification of classic apoptosis through caspase-3 positivity and the elucidation of RIPK1-mediated mechanisms [12]. Utilizing a proinflammatory cocktail of TNF-α, IL-6, and IL-1β to mimic the inflammatory environment of inflammatory bowel disease (IBD), we observed clear differences in the cellular responses to acute versus chronic inflammation [11]. Light microscopy (Fig. 4) and immunofluorescence (Fig. 5) of intestinal organoids derived from patients with Hirschsprung's disease (HSCR) demonstrated profound structural alterations under proinflammatory conditions. Initially, the organoids exhibited well-defined crypt structures and complex morphology. However, acute proinflammatory stimulation led to a marked increase in cell death, indicated by nuclear destruction and a loss of cellular outlines. Chronic stimulation exacerbated this effect, resulting in a significant reduction in structural complexity, with organoids becoming rounded and developing thicker walls. HSCR organoids displayed considerable disintegration and cell death. These observations indicate that HSCR organoids have a unique and compromised response to inflammatory stress, highlighting an altered epithelial barrier and immune function in the disease. This work not only underscores the vulnerability of HSCR tissues to inflammatory stimuli, but also emphasizes the critical role of inflammatory pathways in the pathophysiology of HSCR.

Under acute conditions, HSCR specimens exhibited an increased number of dead cells (Zombie +) compared to chronic stimulation, a pattern also seen in control specimens. This suggests an adaptive cellular response over time, transitioning toward survival mechanisms. Additionally, although not statistically significant, HSCR tissues had more dead cells than controls, indicating distinct responses to inflammatory challenges in HSCR.

Distinguishing between RIPK1-independent and RIPK1-dependent apoptosis is crucial due to their differing biological implications [13]. RIPK1-independent apoptosis is typically immunologically silent, avoiding an inflammatory response. In contrast, RIPK1 functions as both a kinase and scaffold, balancing cellular survival, apoptosis, and necroptosis [9, 10]. Its activation can shift cellular fate toward inflammatory pathways, especially when influenced by proinflammatory cytokines such as TNF-α, IL-6, and IL-1β [14]. Clinically, aberrant RIPK1 signaling is associated with inflammatory conditions such as IBD, where it regulates the transition of NF-κB signaling from cell survival to apoptosis or necroptosis [9, 10]. This dysregulation disrupts the intestinal barrier, allowing bacterial invasion and leading to enterocolitis. Given the histological similarity between IBD (particularly ulcerative colitis) and HAEC, it is plausible that aberrant RIPK1 signaling also contributes to HAEC pathogenesis [9, 15, 16].

Table 3 Effects of treatment on the apoptotic and necroptotic pathways in Zombie + (dead) cells across chronic and acute HSCR and CO groups

Zombie status	Analysis group	Group	Measurement	Key findings	*p* value
Dead ($Zombie^+$)	Chronic	HSCR	RIPK1-apoptosis ($RIP3^+/caspase\text{-}3^+$)	↓After treatment	0.0026
Dead ($Zombie^+$)	Chronic	CO	RIPK1-apoptosis ($RIP3^+/caspase\text{-}3^+$)	↓After treatment	0.0407
Dead ($Zombie^+$)	Acute	HSCR	Apoptosis ($RIP3^-/caspase\text{-}3^+$)	↑After treatment	0.0220
Dead ($Zombie^+$)	Chronic	HSCR	Apoptosis ($RIP3^-/caspase\text{-}3^+$)	↑After treatment	0.0158
Dead ($Zombie^+$)	Chronic	CO	Apoptosis ($RIP3^-/caspase\text{-}3^+$)	↑After treatment	0.0159
Dead ($Zombie^+$)	Acute	CO	Necroptosis ($RIP3^+/caspase\text{-}3^-$)	↓After treatment	0.0182

Table 4 Impact of treatment on apoptosis in Zombie − (alive) cells in acute HSCR and chronic CO groups

Zombie status	Analysis group	Group	Measurement	Key findings	*P* value
Alive ($Zombie^-$)	Acute	HSCR	Apoptosis ($RIP3^-/caspase\text{-}3^+$)	↑After treatment	0.0474
Alive ($Zombie^-$)	Chronic	CO	Apoptosis ($RIP3^-/caspase\text{-}3^+$)	↑After treatment	0.0101

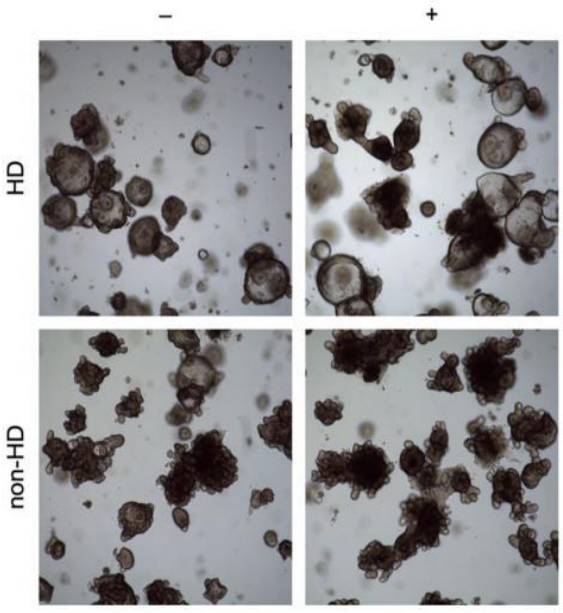

Fig. 4 Light microscopy images of intestinal organoids from two patients, one suffering from Hirschsprung's disease (HSCR) and one serving as non-HSCR control, before and after acute proinflammatory treatment. Tissue specimens prepared from colon sections, ganglionic in case of HSCR. Mucosa preparation, organoid isolation, and culture treatment were performed as described. Magnification 4×. Images taken with a Leica DM IL LED microscope. Acute proinflammatory stimulation results in increased cell death with disintegration of organoid structure and signs of cell death. Complexity of overall organoids morphology as seen before stimulation is mainly maintained

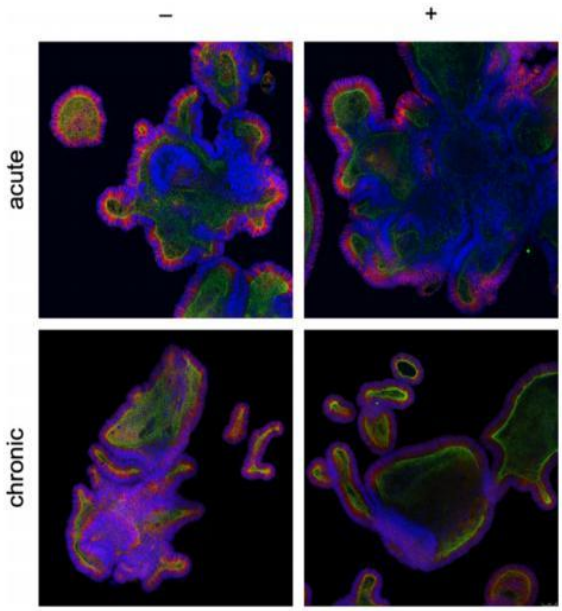

Fig. 5 Immunofluorescence microscopy of intestinal organoids from a patient with Morbus Hirschsprung. Tissue specimens prepared from ganglionic colon section. Mucosa preparation, organoid isolation, and culture treatment were performed as described. Outlining of the organoids marked by intestinal barrier markers beta-catenin (red) and ZO-1 (green), nuclei stained with DAPI (blue) for orientation. Magnification 20×, images taken with the Olympus FV 3000 (acute) and Leica SP5 (chronic) confocal microscopes. Before stimulation, enteroids present with defined crypt structures and complex morphology. Acute treatment with proinflammatory cytokines leads to increased cell death, seen by nuclei destruction and loss of outlines. Following chronic treatment, organoids lost most of the crypt structure complexity and presented round with thickened wall diameter

In the context of HSCR and HAEC, altered apoptotic pathways may explain the differential responses to inflammatory stimuli. Our study shows that in HSCR, cells are more inclined towardsRIPK1-dependent apoptosis, which can link to proinflammatory signaling. This contrasts with the cellular environment in healthy controls, where apoptosis occurs in a more RIPK1-independent manner, often avoiding inflammatory escalation [17]. Furthermore, serum-derived exosomal microRNA-18a-5p has been shown to promote apoptosis in HAEC through the suppression of RORA and regulation of the SIRT1/NFκB pathway, creating a proinflammatory microenvironment [18]. Additionally, disruptions in neuroimmune regulation have been observed, suggesting a complex interplay between nerve cells and immune cells in HAEC, which could further drive the unique apoptotic landscape in these patients [19]. This evidence underscores that in HSCR, apoptosis and its regulation via RIPK1 may play a more prominent role in the pathogenesis of HAEC, diverging significantly from the mechanisms observed in healthy controls.

Understanding the dynamics between viable and non-viable cells is crucial, especially in how a proinflammatory stimulus can activate different cell death pathways within the same cell. A viable cell, despite initiating cell death processes, may initially balance these mechanisms depending on factors like RIPK1 availability. Over time, this balance shifts toward non-viability, progressing through apoptosis or necroptosis. Our analysis showed that viable cells in the HSCR group more frequently underwent RIPK1-dependent apoptosis, especially under chronic stress, whereas control group cells showed no difference between acute and chronic conditions. This suggests a cellular shift in HSCR toward classic apoptosis when RIPK1 becomes less available over time upon proinflammatory stimulation (Table 3**,** Fig. 3v). In non-viable cells, a more pronounced regulatory role for RIPK1 was observed, as evidenced by a decrease in RIPK1-dependent apoptosis upon chronic stimulation. This adaptive modulation in apoptotic pathways indicates that cells, under prolonged stress, may recalibrate their mechanisms to avoid the inflammatory pathways initially triggered by RIPK1 [20]. This shift could represent an attempt by the tissue to adapt to sustained damage or a progression toward a more critical pathological state [21].

The low presence of necroptotic cells (RIPK3 + /caspase-3−) across both HSCR and control groups further emphasizes that necroptosis, a highly proinflammatory cell death process, plays a subordinate role in this experimental context (Fig. 3C vi). Necroptosis, characterized by cell membrane rupture and subsequent tissue inflammation, is evidently not a major driver of the observed pathology in HSCR or its controls upon stimulation in this setting [13].

Conclusion

In summary, our study highlights the complex interplay of apoptotic pathways in response to inflammatory stimuli in both acute and chronic settings. It emphasizes the importance of considering cell viability when examining cellular responses, particularly in pathological conditions like HSCR and HAEC, where altered apoptosis plays a key role. RIPK1 emerges as a pivotal regulatory protein, influencing the threshold between apoptosis and necroptosis and thereby affecting the overall balance of cell death. This nuanced understanding of cellular adaptation to proinflammatory environments underscores the multifaceted nature of inflammatory responses and opens avenues for further research into the modulation of these pathways for therapeutic benefit.

Acknowledgements The authors like to thank the FACS Sorting Core Facility of the University Medical Center Hamburg-Eppendorf for providing the LSR Fortessa as well as their technical assistance for facilitating this analysis. The responsibility for the content and any remaining errors, omissions, and inaccuracies is our own.

Author's contribution Conceptualization Zhongwen Li, Johanna Hagens and Christian Tomuschat.; methodology Zhongwen Li, Johanna Hagens,Clara Philippi, Laia Pagerols Raluy and Magdalena; formal Analysis Zhongwen Li, Lucie Rohwäder; writing–original draft preparation Zhongwen Li and Christian Tomuschat; writing–review and editing Johanna Hagens, Konrad Reinshagen, Hans Christian Schmidt, Pauline Schuppert, Magdalena Trochimiuk, Laia Pagerols Raluy; visualization Zhongwen Li, Johanna Hagens and Lucie Rohwäder. All authors have read and agreed to the published version of the manuscript.

Funding Open Access funding enabled and organized by Projekt DEAL. The authors would like to acknowledge the Department of Pediatric Surgery of the University Medical Center Hamburg-Eppendorf and especially Prof. Konrad Reinshagen for the financial support. Pauline Schuppert and Hans Christian Schmidt were financially supported by the Else Kröner-Fresenius-Stiftung iPRIME Scholarship (2021_EKPK.10), UKE, Hamburg. The authors certify that they have no affiliations with or involvement in any organization or entity with any financial interest or non-financial interest in the subject matter or materials discussed in this manuscript.

Declarations

Conflict of interest The authors declare that the research was conducted in the absence of any commercial or financial relationships that could be construed as a potential conflict of interest.

Ethical approval The studies involving humans were approved by the Institutional Review Board Hamburg ethics committee (PV5251). The studies were conducted in accordance with the local legislation and institutional requirements. The participants provided their written informed consent to participate in this study.

Content of publisher All claims expressed in this article are solely those of the authors and do not necessarily represent those of their affiliated organizations, or those of the publisher, the editors, and the reviewers. Any product that may be evaluated in this article, or claim that may be made by its manufacturer, is not guaranteed or endorsed by the publisher.

Data availability The original contributions presented in the study are included in the article/Supplementary Material. Further inquiries can be directed to Christian Tomuschat.

References

1. Tilghman JM, Ling AY, Turner TN et al (2019) Molecular genetic anatomy and risk profile of Hirschsprung's disease. N Engl J Med 380:1421–1432. https://doi.org/10.1056/nejmoa1706594
2. Thakkar HS, Blackburn S, Curry J et al (2020) Variability of the transition zone length in Hirschsprung disease. J Pediatr Surg 55:63–66. https://doi.org/10.1016/j.jpedsurg.2019.09.056
3. Kyrklund K, Sloots CEJ, de Blaauw I et al (2020) ERNICA guidelines for the management of rectosigmoid Hirschsprung's disease. Orphanet J Rare Dis. https://doi.org/10.1186/s13023-020-01362-3
4. Bernstein CN, Kuenzig ME, Coward S et al (2021) Increased incidence of inflammatory bowel disease after Hirschsprung disease: a population-based cohort study. J Pediatr 233:98-104.e2. https://doi.org/10.1016/j.jpeds.2021.01.060
5. Gershon EM, Rodriguez L, Arbizu RA (2023) Hirschsprung's disease associated enterocolitis: a comprehensive review. World J Clin Pediatr 12:68–76. https://doi.org/10.5409/wjcp.v12.i3.68
6. Hagens J, Reinshagen K, Tomuschat C (2021) Prevalence of Hirschsprung-associated enterocolitis in patients with Hirschsprung disease. Pediatr Surg Int. https://doi.org/10.1007/s00383-021-05020-y
7. Nakamura H, Lim T, Puri P (2018) Inflammatory bowel disease in patients with Hirschsprung's disease: a systematic review and meta-analysis. Pediatr Surg Int. https://doi.org/10.1007/s00383-017-4182-4
8. Granström AL, Amin L, Arnell H, Wester T (2018) Increased risk of inflammatory bowel disease in a population-based cohort study of patients with Hirschsprung disease. J Pediatr Gastroenterol Nutr 66:398–401. https://doi.org/10.1097/MPG.0000000000001732
9. Kondylis V, Kumari S, Vlantis K, Pasparakis M (2017) The interplay of IKK, NF-κB and RIPK1 signaling in the regulation of cell death, tissue homeostasis and inflammation. Immunol Rev 277:113–127
10. Wong J, Garcia-Carbonell R, Zelic M et al (2020) RIPK1 mediates TNF-induced intestinal crypt apoptosis during chronic NF-κB activation. Cmgh 9:295–312. https://doi.org/10.1016/j.jcmgh.2019.10.002
11. d'Aldebert E, Quaranta M, Sébert M et al (2020) Characterization of human colon organoids from inflammatory bowel disease patients. Front Cell Dev Biol 8:363. https://doi.org/10.3389/fcell.2020.00363
12. Lee HL, Pike R, Chong MHA et al (2018) Simultaneous flow cytometric immunophenotyping of necroptosis, apoptosis and RIP1-dependent apoptosis. Methods 134–135:56–66. https://doi.org/10.1016/j.ymeth.2017.10.013
13. Günther C, Neumann H, Neurath MF, Becker C (2013) Apoptosis, necrosis and necroptosis: cell death regulation in the intestinal epithelium. Gut 62:1062–1071. https://doi.org/10.1136/gutjnl-2011-301364
14. van Loo G, Bertrand MJM (2023) Death by TNF: a road to inflammation. Nat Rev Immunol 23:289–303. https://doi.org/10.1038/s41577-022-00792-3
15. Austin KM (2012) The pathogenesis of Hirschsprung's disease-associated enterocolitis. Semin Pediatr Surg. https://doi.org/10.1053/j.sempedsurg.2012.07.006
16. Vlantis K, Wullaert A, Polykratis A et al (2016) NEMO prevents RIP Kinase 1-mediated epithelial cell death and chronic intestinal inflammation by NF-κB-dependent and -independent functions. Immunity 44:553–567. https://doi.org/10.1016/j.immuni.2016.02.020
17. Li H, Zhou L, Zhi Z et al (2020) Lipopolysaccharide upregulates miR-132/212 in Hirschsprung-associated enterocolitis, facilitating pyroptosis by activating NLRP3 inflammasome via targeting Sirtuin 1 (SIRT1). Aging 12:18588–18602. https://doi.org/10.18632/aging.103852
18. Chen Y, Yuan X, Li Y et al (2021) Circulating exosomal microRNA-18a-5p accentuates intestinal inflammation in Hirschsprung-associated enterocolitis by targeting RORA. Am J Transl Res 13:4182–4196
19. Ji H, Lai D, Tou J (2023) Neuroimmune regulation in Hirschsprung's disease associated enterocolitis. Front Immunol 14:1127375. https://doi.org/10.3389/fimmu.2023.1127375
20. Pasparakis M, Vandenabeele P (2015) Necroptosis and its role in inflammation. Nature 517:311–320. https://doi.org/10.1038/nature14191
21. Newton K, Dugger DL, Wickliffe KE et al (2014) Activity of protein kinase RIPK3 determines whether cells die by necroptosis or apoptosis. Science 343:1357–1360. https://doi.org/10.1126/science.124936

3. Zusammenfassung

Unsere Studie zeigt, wie organ-spezifisch Organoide bei Morbus Hirschsprung (HSCR) auf akute und chronische Entzündungsreize reagieren. Dabei konnten wir mittels eines neu etablierten FACS-basierten Assays unterschiedliche Formen des programmierten Zelltods (RIPK1-abhängige und -unabhängige Apoptose sowie Nekroptose) in lebenden und toten Zellen identifizieren und analysieren.

Unter akuter Stimulation zeigten HSCR-Organoide eine erhöhte Zellsterblichkeit im Vergleich zu Kontrollen. Bei chronischer Stimulation kam es zu einer Verschiebung der Zelltodmechanismen: Während die RIPK1-abhängige Apoptose abnahm, nahmen alternative Signalwege – insbesondere RIPK1-unabhängige – zu. Diese dynamische Umstellung lässt auf eine adaptive, jedoch gestörte epithelial-immunologische Antwort schließen.

RIPK1 fungiert dabei als zentraler Regulator zwischen immunologisch stiller Apoptose und entzündungsfördernder Nekroptose. Die Ergebnisse unterstreichen die Bedeutung dieses Signalwegs im epithelialen Stressverhalten und liefern neue Hinweise auf krankheitsspezifische Besonderheiten bei HSCR.

Diese Erkenntnisse könnten dazu beitragen, pathologische Entzündungsreaktionen bei HSCR besser zu verstehen und neue therapeutische Ansätze zur Prävention von HAEC zu entwickeln.

Abstract

Background:Hirschsprung's disease (HSCR) is a congenital disorder of the enteric nervous system that predisposes patients to severe inflammatory complications, such as Hirschsprung-associated enterocolitis (HAEC).

Method:In this study, we employed a novel flow cytometry-based assay to investigate the dynamics of cell death in colonic organoids from HSCR patients and matched controls subjected to acute and chronic inflammatory stimuli.

Main Result:Using this approach, we quantified three distinct types of programmed cell death — RIPK1-dependent apoptosis, RIPK1-independent apoptosis, and necroptosis — in both viable and non-viable cells. Our data revealed that HSCR organoids exhibited a significantly increased susceptibility to acute inflammation, with elevated rates of cell death compared to controls. In contrast, chronic stimulation induced a regulatory shift from RIPK1-dependent to RIPK1-independent apoptosis, particularly in non-viable HSCR cells.These results, derived from patient-specific organoid models, provide insight into the epithelial stress response in HSCR.

Conclusion:These findings suggest altered inflammatory signaling in HSCR and highlight the central role of RIPK1 in regulating epithelial cell fate, and may guide the development of targeted therapeutic strategies for preventing HAEC in patients with HSCR.

4. Reference

Austin K. M. (2012). The pathogenesis of Hirschsprung's disease-associated enterocolitis. Seminars in pediatric surgery, 21(4), 319 – 327. https://doi.org/10.1053/j.sempedsurg.2012.07.006.

Bernstein, C. N., Kuenzig, M. E., Coward, S., Nugent, Z., Nasr, A., El-Matary, W., Singh, H., Kaplan, G. G., & Benchimol, E. I. (2021). Increased Incidence of Inflammatory Bowel Disease After Hirschsprung Disease: A Population-based Cohort Study. The Journal of pediatrics, 233, 98–104.e2. https://doi.org/10.1016/j.jpeds.2021.01.060

Chen, Y., Yuan, X., Li, Y., Chen, J., Wu, S., Jiang, A., Miao, X., & Shu, Q. (2021). Circulating exosomal microRNA-18a-5p accentuates intestinal inflammation in Hirschsprung-associated enterocolitis by targeting RORA. American journal of translational research, 13(5), 4182–4196.

d'Aldebert, E., Quaranta, M., Sébert, M., Bonnet, D., Kirzin, S., Portier, G., Duffas, J. P., Chabot, S., Lluel, P., Allart, S., Ferrand, A., Alric, L., Racaud-Sultan, C., Mas, E., Deraison, C., & Vergnolle, N. (2020). Characterization of Human Colon Organoids From Inflammatory Bowel Disease Patients. Frontiers in cell and developmental biology, 8, 363. https://doi.org/10.3389/fcell.2020.00363

Gershon, E. M., Rodriguez, L., & Arbizu, R. A. (2023). Hirschsprung's disease associated enterocolitis: A comprehensive review. World journal of clinical pediatrics, 12(3), 68–76. https://doi.org/10.5409/wjcp.v12.i3.68

Günther, C., Neumann, H., Neurath, M. F., & Becker, C. (2013). Apoptosis, necrosis and necroptosis: cell death regulation in the intestinal epithelium. Gut, 62(7), 1062–1071. https://doi.org/10.1136/gutjnl-2011-301364

Hagens, J., Reinshagen, K., & Tomuschat, C. (2022). Prevalence of Hirschsprung-associated enterocolitis in patients with Hirschsprung disease. Pediatric surgery international, 38(1), 3–24. https://doi.org/10.1007/s00383-021-05020-y

JJi, H., Lai, D., & Tou, J. (2023). Neuroimmune regulation in Hirschsprung's disease associated enterocolitis. Frontiers in immunology, 14, 1127375. https://doi.org/10.3389/fimmu.2023.1127375

Kondylis, V., Kumari, S., Vlantis, K., & Pasparakis, M. (2017). The interplay of IKK, NF-κB and RIPK1 signaling in the regulation of cell death, tissue homeostasis and inflammation. Immunological reviews, 277(1), 113–127. https://doi.org/10.1111/imr.12550

Lee, H. L., Pike, R., Chong, M. H. A., Vossenkamper, A., & Warnes, G. (2018). Simultaneous flow cytometric immunophenotyping of necroptosis, apoptosis and RIP1-dependent apoptosis. Methods (San Diego, Calif.), 134-135, 56 – 66. https://doi.org/10.1016/j.ymeth.2017.10.013

Lu, H., Li, H., Fan, C., Qi, Q., Yan, Y., Wu, Y., Feng, C., Wu, B., Gao, Y., Zuo, J., & Tang, W. (2020). RIPK1 inhibitor ameliorates colitis by directly maintaining intestinal barrier homeostasis and regulating following IECs-immuno crosstalk. Biochemical pharmacology, 172, 113751. https://doi.org/10.1016/j.bcp.2019.113751

Newton, K., Dugger, D. L., Wickliffe, K. E., Kapoor, N., de Almagro, M. C., Vucic, D., Komuves, L., Ferrando, R. E., French, D. M., Webster, J., Roose-Girma, M., Warming, S., & Dixit, V. M. (2014). Activity of protein kinase RIPK3 determines whether cells die by necroptosis or apoptosis. Science (New York, N.Y.), 343(6177), 1357 – 1360. https://doi.org/10.1126/science.1249361

Pasparakis, M., Vandenabeele, P.(2015). Necroptosis and its role in inflammation. *Nature,*517, 311–320. https://doi.org/10.1038/nature14191

van Loo, G., & Bertrand, M. J. M. (2023). Death by TNF: a road to inflammation. Nature reviews. Immunology, 23(5), 289–303. https://doi.org/10.1038/s41577-022-00792-3

Vlantis, K., Wullaert, A., Polykratis, A., Kondylis, V., Dannappel, M., Schwarzer, R., Welz, P., Corona, T., Walczak, H., Weih, F., Klein, U., Kelliher, M., & Pasparakis, M. (2016). NEMO Prevents RIP Kinase 1-Mediated Epithelial Cell Death and Chronic Intestinal Inflammation by NF-κB-Dependent and -Independent Functions. Immunity, 44(3), 553–567. https://doi.org/10.1016/j.immuni.2016.02.020

Wong, J., Garcia-Carbonell, R., Zelic, M., Ho, S. B., Boland, B. S., Yao, S. J., Desai, S. A., Das, S., Planell, N., Harris, P. A., Font-Burgada, J., Taniguchi, K., Bertin, J., Salas, A., Pasparakis, M., Gough, P. J., Kelliher, M., Karin, M., & Guma, M. (2020). RIPK1 Mediates TNF-Induced Intestinal Crypt Apoptosis During Chronic NF-κB Activation. Cellular and molecular gastroenterology and hepatology, 9(2), 295 – 312. https://doi.org/10.1016/j.jcmgh.2019.10.00202

5. List of Abbreviations

CO	Control Group
FSC-A	Forward Scatter-Area
HAEC	Hirschsprung-associated enterocolitis
HSCR	Hirschsprung's Disease
IBD	Inflammatory Bowel Disease
IL-1β	Interleukin 1 beta
IL-6	Interleukin 6
ODM-h	Organoid Differentiation Medium Human
OGM-h	Organoid Growth Medium Human
RIPK1	Receptor-Interacting Protein Kinase 1
RIPK3	Receptor-Interacting Protein Kinase 3
SSC-A	Side Scatter-Area
TNFR1	Tumor necrosis factor receptor 1
TNF-α	Tumor Necrosis Factor alpha

6. List of Figures

7. List of Tables

8. Authors' contribution

Contribution	Authors
Conceptualization	Zhongwen Li, Johanna Hagens, Christian Tomuschat
Methodology	Zhongwen Li, Johanna Hagens, Clara Philippi, Laia Pagerols Raluy, Magdalena
Formal Analysis	Zhongwen Li
Writing – Original Draft	Zhongwen Li, Christian Tomuschat
Writing – Review & Editing	Johanna Hagens, Konrad Reinshagen, Hans Christian Schmidt, Pauline Schuppert, Magdalena Trochimiuk, Laia Pagerols Raluy
Visualization	Zhongwen Li, Johanna Hagens

All authors have read and agreed to the published version of the manuscrip.

9. Eidesstattliche Versicherung

Ich versichere ausdrücklich, dass ich die Arbeit selbständig und ohne fremde Hilfe, insbesondere ohne entgeltliche Hilfe von Vermittlungs- und Beratungsdiensten, verfasst, andere als die von mir angegebenen Quellen und Hilfsmittel nicht benutzt und die aus den benutzten Werken wörtlich oder inhaltlich entnommenen Stellen einzeln nach Ausgabe (Auflage und Jahr des Erscheinens), Band und Seite des benutzten Werkes kenntlich gemacht habe. Das gilt insbesondere auch für alle Informationen aus Internetquellen.

Soweit beim Verfassen der Dissertation KI-basierte Tools („Chatbots“) verwendet wurden, versichere ich ausdrücklich, den daraus generierten Anteil deutlich kenntlich gemacht zu haben. Die „Stellungnahme des Präsidiums der Deutschen Forschungsgemeinschaft (DFG) zum Einfluss generativer Modelle für die Text- und Bilderstellung auf die Wissenschaften und das Förderhandeln der DFG“ aus September 2023 wurde dabei beachtet.

Ferner versichere ich, dass ich die Dissertation bisher nicht einem Fachvertreter an einer anderen Hochschule zur Überprüfung vorgelegt oder mich anderweitig um Zulassung zur Promotion beworben habe.

Ich erkläre mich damit einverstanden, dass meine Dissertation vom Dekanat der Medizinischen Fakultät mit einer gängigen Software zur Erkennung von Plagiaten überprüft werden kann.

Datum 10.07.2025 Unterschrift Zhongwen Li

10. Acknowledgements

I would first like to express my heartfelt gratitude to my supervisors, Prof. Dr. Christian Tomuschat and Prof. Dr. Konrad Reinshagen, for giving me the opportunity to pursue my doctoral studies under their guidance. Your unwavering support, both academically and personally, has been invaluable. I truly appreciate your patience, insightful advice on research methodology, and the detailed feedback on my academic writing, all of which have shaped me into a better researcher. I am also sincerely grateful for entrusting me with such a fascinating research topic and for involving me in other meaningful collaborative projects that have significantly broadened my academic horizons.

My special thanks go to Dr. Laia Pagerols Raluy for her dedicated assistance with statistical analysis and her valuable contributions to the manuscript writing and revision process.

I am also thankful to Johanna Hagens, Hans Christian Schmidt, Pauline Schuppert, and Magdalena Trochimiuk for their kindness, support, and warm companionship throughout these three years, which truly made me feel at home.

I gratefully acknowledge the FACS Sorting Core Facility at the University Medical Center Hamburg-Eppendorf for providing the LSR Fortessa and for their technical assistance during the analysis. Any remaining errors or inaccuracies are solely my responsibility.

I deeply appreciate the generous scholarship provided by the China Scholarship Council (CSC), which made it possible for me to study in Germany. I would also like to extend my thanks to the Chinese Consulate in Hamburg for their essential support in medical and safety matters during my stay.

Finally, my deepest gratitude goes to my parents, whose constant love and unwavering support — despite the distance and time difference — have been my greatest source of strength throughout this journey.